Search for Acoplanar Lepton Pair Events in e$^+$e$^-$ Collisions at $\sqrt{s} = 161$, 172 and 183 GeV

The OPAL Collaboration

Abstract

A selection of di-lepton events with significant missing transverse momentum has been performed using a total data sample of 77.0 pb^{-1} at e$^+$e$^-$ centre-of-mass energies of 161 GeV, 172 GeV and 183 GeV. The observed numbers of events: four at 161 GeV, nine at 172 GeV, and 78 at 183 GeV, are consistent with the numbers expected from Standard Model processes, which arise predominantly from W$^+$W$^-$ production with each W decaying leptonically. This topology is an experimental signature also for the pair production of new particles that decay to a charged lepton accompanied by one or more invisible particles. Further event selection criteria are described that optimise the sensitivity to particular new physics channels. No evidence for new phenomena is apparent and model independent limits on the production cross-section times branching ratio squared for various new physics processes are presented. Assuming a 100% branching ratio for the decay $\tilde{\ell}_R^\pm \to \ell^\pm \tilde{\chi}_1^0$, we exclude at 95% CL: right-handed smuons with masses below 65 GeV for $m_{\tilde{\mu}^-} - m_{\tilde{\chi}_1^0} > 2$ GeV and right-handed staus with masses below 64 GeV for $m_{\tilde{\tau}^-} - m_{\tilde{\chi}_1^0} > 10$ GeV. Right-handed selectrons are excluded at 95% CL for masses below 77 GeV for $m_{\tilde{e}^-} - m_{\tilde{\chi}_1^0} > 5$ GeV within the framework of the Minimal Supersymmetric Standard Model assuming $\mu < -100$ GeV and $\tan\beta = 1.5$.

(Submitted to Eur. Phys. J. C.)

G. Abbiendi[2], K. Ackerstaff[8], G. Alexander[23], J. Allison[16], N. Altekamp[5], K.J. Anderson[9],
S. Anderson[12], S. Arcelli[17], S. Asai[24], S.F. Ashby[1], D. Axen[29], G. Azuelos[18,a], A.H. Ball[17],
E. Barberio[8], R.J. Barlow[16], R. Bartoldus[3], J.R. Batley[5], S. Baumann[3], J. Bechtluft[14],
T. Behnke[27], K.W. Bell[20], G. Bella[23], A. Bellerive[9], S. Bentvelsen[8], S. Bethke[14], S. Betts[15],
O. Biebel[14], A. Biguzzi[5], S.D. Bird[16], V. Blobel[27], I.J. Bloodworth[1], M. Bobinski[10], P. Bock[11],
J. Böhme[14], D. Bonacorsi[2], M. Boutemeur[34], S. Braibant[8], P. Bright-Thomas[1], L. Brigliadori[2],
R.M. Brown[20], H.J. Burckhart[8], C. Burgard[8], R. Bürgin[10], P. Capiluppi[2], R.K. Carnegie[6],
A.A. Carter[13], J.R. Carter[5], C.Y. Chang[17], D.G. Charlton[1,b], D. Chrisman[4], C. Ciocca[2],
P.E.L. Clarke[15], E. Clay[15], I. Cohen[23], J.E. Conboy[15], O.C. Cooke[8], C. Couyoumtzelis[13],
R.L. Coxe[9], M. Cuffiani[2], S. Dado[22], G.M. Dallavalle[2], R. Davis[30], S. De Jong[12], L.A. del Pozo[4],
A. de Roeck[8], K. Desch[8], B. Dienes[33,d], M.S. Dixit[7], J. Dubbert[34], E. Duchovni[26], G. Duckeck[34],
I.P. Duerdoth[16], D. Eatough[16], P.G. Estabrooks[6], E. Etzion[23], H.G. Evans[9], F. Fabbri[2],
M. Fanti[2], A.A. Faust[30], F. Fiedler[27], M. Fierro[2], I. Fleck[8], R. Folman[26], A. Fürtjes[8],
D.I. Futyan[16], P. Gagnon[7], J.W. Gary[4], J. Gascon[18], S.M. Gascon-Shotkin[17], G. Gaycken[27],
C. Geich-Gimbel[3], G. Giacomelli[2], P. Giacomelli[2], V. Gibson[5], W.R. Gibson[13],
D.M. Gingrich[30,a], D. Glenzinski[9], J. Goldberg[22], W. Gorn[4], C. Grandi[2], E. Gross[26],
J. Grunhaus[23], M. Gruwé[27], G.G. Hanson[12], M. Hansroul[8], M. Hapke[13], K. Harder[27],
C.K. Hargrove[7], C. Hartmann[3], M. Hauschild[8], C.M. Hawkes[5], R. Hawkings[27],
R.J. Hemingway[6], M. Herndon[17], G. Herten[10], R.D. Heuer[8], M.D. Hildreth[8], J.C. Hill[5],
S.J. Hillier[1], P.R. Hobson[25], A. Hocker[9], R.J. Homer[1], A.K. Honma[28,a], D. Horváth[32,c],
K.R. Hossain[30], R. Howard[29], P. Hüntemeyer[27], P. Igo-Kemenes[11], D.C. Imrie[25], K. Ishii[24],
F.R. Jacob[20], A. Jawahery[17], H. Jeremie[18], M. Jimack[1], C.R. Jones[5], P. Jovanovic[1], T.R. Junk[6],
D. Karlen[6], V. Kartvelishvili[16], K. Kawagoe[24], T. Kawamoto[24], P.I. Kayal[30], R.K. Keeler[28],
R.G. Kellogg[17], B.W. Kennedy[20], A. Klier[26], S. Kluth[8], T. Kobayashi[24], M. Kobel[3,e],
D.S. Koetke[6], T.P. Kokott[3], M. Kolrep[10], S. Komamiya[24], R.V. Kowalewski[28], T. Kress[11],
P. Krieger[6], J. von Krogh[11], T. Kuhl[3], P. Kyberd[13], G.D. Lafferty[16], D. Lanske[14], J. Lauber[15],
S.R. Lautenschlager[31], I. Lawson[28], J.G. Layter[4], D. Lazic[22], A.M. Lee[31], D. Lellouch[26],
J. Letts[12], L. Levinson[26], R. Liebisch[11], B. List[8], C. Littlewood[5], A.W. Lloyd[1], S.L. Lloyd[13],
F.K. Loebinger[16], G.D. Long[28], M.J. Losty[7], J. Ludwig[10], D. Liu[12], A. Macchiolo[2],
A. Macpherson[30], W. Mader[3], M. Mannelli[8], S. Marcellini[2], C. Markopoulos[13], A.J. Martin[13],
J.P. Martin[18], G. Martinez[17], T. Mashimo[24], P. Mättig[26], W.J. McDonald[30], J. McKenna[29],
E.A. Mckigney[15], T.J. McMahon[1], R.A. McPherson[28], F. Meijers[8], S. Menke[3], F.S. Merritt[9],
H. Mes[7], J. Meyer[27], A. Michelini[2], S. Mihara[24], G. Mikenberg[26], D.J. Miller[15], R. Mir[26],
W. Mohr[10], A. Montanari[2], T. Mori[24], K. Nagai[8], I. Nakamura[24], H.A. Neal[12], B. Nellen[3],
R. Nisius[8], S.W. O'Neale[1], F.G. Oakham[7], F. Odorici[2], H.O. Ogren[12], M.J. Oreglia[9], S. Orito[24],
J. Pálinkás[33,d], G. Pásztor[32], J.R. Pater[16], G.N. Patrick[20], J. Patt[10], R. Perez-Ochoa[8],
S. Petzold[27], P. Pfeifenschneider[14], J.E. Pilcher[9], J. Pinfold[30], D.E. Plane[8], P. Poffenberger[28],
J. Polok[8], M. Przybycień[8], C. Rembser[8], H. Rick[8], S. Robertson[28], S.A. Robins[22], N. Rodning[30],
J.M. Roney[28], K. Roscoe[16], A.M. Rossi[2], Y. Rozen[22], K. Runge[10], O. Runolfsson[8], D.R. Rust[12],
K. Sachs[10], T. Saeki[24], O. Sahr[34], W.M. Sang[25], E.K.G. Sarkisyan[23], C. Sbarra[29], A.D. Schaile[34],
O. Schaile[34], F. Scharf[3], P. Scharff-Hansen[8], J. Schieck[11], B. Schmitt[8], S. Schmitt[11],
A. Schöning[8], M. Schröder[8], M. Schumacher[3], C. Schwick[8], W.G. Scott[20], R. Seuster[14],
T.G. Shears[8], B.C. Shen[4], C.H. Shepherd-Themistocleous[8], P. Sherwood[15], G.P. Siroli[2],
A. Sittler[27], A. Skuja[17], A.M. Smith[8], G.A. Snow[17], R. Sobie[28], S. Söldner-Rembold[10],
M. Sproston[20], A. Stahl[3], K. Stephens[16], J. Steuerer[27], K. Stoll[10], D. Strom[19], R. Ströhmer[34],
B. Surrow[8], S.D. Talbot[1], S. Tanaka[24], P. Taras[18], S. Tarem[22], R. Teuscher[8], M. Thiergen[10],
M.A. Thomson[8], E. von Törne[3], E. Torrence[8], S. Towers[6], I. Trigger[18], Z. Trócsányi[33],

1

E. Tsur[23], A.S. Turcot[9], M.F. Turner-Watson[8], R. Van Kooten[12], P. Vannerem[10],
M. Verzocchi[10], H. Voss[3], F. Wäckerle[10], A. Wagner[27], C.P. Ward[5], D.R. Ward[5], P.M. Watkins[1],
A.T. Watson[1], N.K. Watson[1], P.S. Wells[8], N. Wermes[3], J.S. White[6], G.W. Wilson[16],
J.A. Wilson[1], T.R. Wyatt[16], S. Yamashita[24], G. Yekutieli[26], V. Zacek[18], D. Zer-Zion[8]

[1]School of Physics and Astronomy, University of Birmingham, Birmingham B15 2TT, UK
[2]Dipartimento di Fisica dell' Università di Bologna and INFN, I-40126 Bologna, Italy
[3]Physikalisches Institut, Universität Bonn, D-53115 Bonn, Germany
[4]Department of Physics, University of California, Riverside CA 92521, USA
[5]Cavendish Laboratory, Cambridge CB3 0HE, UK
[6]Ottawa-Carleton Institute for Physics, Department of Physics, Carleton University, Ottawa,
Ontario K1S 5B6, Canada
[7]Centre for Research in Particle Physics, Carleton University, Ottawa, Ontario K1S 5B6,
Canada
[8]CERN, European Organisation for Particle Physics, CH-1211 Geneva 23, Switzerland
[9]Enrico Fermi Institute and Department of Physics, University of Chicago, Chicago IL 60637,
USA
[10]Fakultät für Physik, Albert Ludwigs Universität, D-79104 Freiburg, Germany
[11]Physikalisches Institut, Universität Heidelberg, D-69120 Heidelberg, Germany
[12]Indiana University, Department of Physics, Swain Hall West 117, Bloomington IN 47405,
USA
[13]Queen Mary and Westfield College, University of London, London E1 4NS, UK
[14]Technische Hochschule Aachen, III Physikalisches Institut, Sommerfeldstrasse 26-28, D-52056
Aachen, Germany
[15]University College London, London WC1E 6BT, UK
[16]Department of Physics, Schuster Laboratory, The University, Manchester M13 9PL, UK
[17]Department of Physics, University of Maryland, College Park, MD 20742, USA
[18]Laboratoire de Physique Nucléaire, Université de Montréal, Montréal, Quebec H3C 3J7,
Canada
[19]University of Oregon, Department of Physics, Eugene OR 97403, USA
[20]CLRC Rutherford Appleton Laboratory, Chilton, Didcot, Oxfordshire OX11 0QX, UK
[22]Department of Physics, Technion-Israel Institute of Technology, Haifa 32000, Israel
[23]Department of Physics and Astronomy, Tel Aviv University, Tel Aviv 69978, Israel
[24]International Centre for Elementary Particle Physics and Department of Physics, University
of Tokyo, Tokyo 113, and Kobe University, Kobe 657, Japan
[25]Institute of Physical and Environmental Sciences, Brunel University, Uxbridge, Middlesex
UB8 3PH, UK
[26]Particle Physics Department, Weizmann Institute of Science, Rehovot 76100, Israel
[27]Universität Hamburg/DESY, II Institut für Experimental Physik, Notkestrasse 85, D-22607
Hamburg, Germany
[28]University of Victoria, Department of Physics, P O Box 3055, Victoria BC V8W 3P6, Canada
[29]University of British Columbia, Department of Physics, Vancouver BC V6T 1Z1, Canada
[30]University of Alberta, Department of Physics, Edmonton AB T6G 2J1, Canada
[31]Duke University, Dept of Physics, Durham, NC 27708-0305, USA
[32]Research Institute for Particle and Nuclear Physics, H-1525 Budapest, P O Box 49, Hungary
[33]Institute of Nuclear Research, H-4001 Debrecen, P O Box 51, Hungary

^{34}Ludwigs-Maximilians-Universität München, Sektion Physik, Am Coulombwall 1, D-85748 Garching, Germany

^{a} and at TRIUMF, Vancouver, Canada V6T 2A3
^{b} and Royal Society University Research Fellow
^{c} and Institute of Nuclear Research, Debrecen, Hungary
^{d} and Department of Experimental Physics, Lajos Kossuth University, Debrecen, Hungary
^{e} on leave of absence from the University of Freiburg

1   Introduction

We report on the selection of events containing two charged leptons and significant missing transverse momentum. Data are analysed at e^+e^- centre-of-mass energies of 161, 172 and 183[1] GeV with integrated luminosities corresponding to 10.3 pb^{-1}, 10.3 pb^{-1} and 56.4 pb^{-1}, respectively. The number and properties of the observed events are found to be consistent with the expectations for Standard Model processes, which are dominated by the $\ell^+\nu\,\ell^-\overline{\nu}$ final state arising from W^+W^- production in which both W's decay leptonically: $W^- \to \ell^-\overline{\nu}_\ell$.

In most respects the analysis method follows closely our previously published search at 161 and 172 GeV [1]. The event selection is performed in two stages. The first stage consists of a general selection for all the possible events containing a lepton pair plus missing transverse momentum (section 3). In this context the Standard Model $\ell^+\nu\,\ell^-\overline{\nu}$ events are considered as signal in addition to the possible new physics sources. Standard Model processes that do not lead to $\ell^+\nu\,\ell^-\overline{\nu}$ final states — e.g., $e^+e^-\ell^+\ell^-$ and $\ell^+\ell^-(\gamma)$ — are considered as background and are reduced to a rather low level. In the second stage selection the detailed properties of the events are used to separate as far as possible the events consistent with potential new physics sources from W^+W^- and other Standard Model processes (section 4).

In companion papers [2, 3, 4] we use the selected event samples to measure the production of $W^+W^- \to \ell^+\nu\,\ell^-\overline{\nu}$ events. We present here the results of searches for several anomalous sources of such events. We consider the pair production of new particles that decay to produce a charged lepton accompanied by one or more invisible particles, such as neutrinos or the hypothesised lightest stable supersymmetric [5] particle (LSP), which may be the lightest neutralino, $\tilde{\chi}_1^0$, or the gravitino. Specifically, we consider the following new particle decays:

charged scalar leptons (sleptons): $\tilde{\ell}^\pm \to \ell^\pm\tilde{\chi}_1^0$, where $\tilde{\ell}^\pm$ may be a selectron ($\tilde{e}$), smuon ($\tilde{\mu}$) or stau ($\tilde{\tau}$) and $\ell^\pm$ is the corresponding charged lepton.

charged Higgs bosons: $H^\pm \to \tau^\pm\nu_\tau$.

charginos: $\tilde{\chi}_1^\pm \to \ell^\pm\tilde{\nu}$ ("2-body" decays)   or $\tilde{\chi}_1^\pm \to \ell^\pm\nu\tilde{\chi}_1^0$ ("3-body" decays).

Searches for sleptons at LEP2 using this topology have been presented also by other collaborations [6].

In this paper we describe fully only those respects in which the analysis differs significantly from [1]. These are:

- Use of a new subdetector (the MIP plug [7]) to reduce background from four-fermion processes in which a minimum ionizing particle would otherwise have escaped detection in the angular region[2] $60 < \theta(\mathrm{mrad}) < 160$.

- The second stage event selection for smuons, staus and charged Higgs bosons makes use of the charge-signed angular distribution of the observed lepton candidates.

---

[1]In the 1997 LEP run most of the data were collected at e^+e^- centre-of-mass energies of between 181.8 and 183.8 GeV. The luminosity weighted average centre-of-mass energy was 182.7 GeV.

[2]A right-handed coordinate system is adopted, in which the x-axis points to the centre of the LEP ring, and positive z is along the electron beam direction. The angles θ and ϕ are the polar and azimuthal angles, respectively.

- Use of a likelihood technique in the second stage of event selection, to determine whether an event is more consistent with the signal or with the background hypothesis, and applying cuts based on this information.

- In section 6, the 95% CL upper limits on new particle production at $\sqrt{s} = 183$ GeV are obtained by combining the data at the three centre-of-mass energies 161, 172 and 183 GeV using the Likelihood Ratio method [8].

The MIP plug is available only for the data at 183 GeV. The remaining modifications have been applied to the data at all centre-of-mass energies.

2   OPAL Detector and Monte Carlo Simulation

A detailed description of the OPAL detector can be found elsewhere [9].

The central detector consists of a system of tracking chambers providing charged particle tracking over 96% of the full solid angle inside a 0.435 T uniform magnetic field parallel to the beam axis. It consists of a two-layer silicon micro-strip vertex detector, a high precision drift chamber, a large volume jet chamber and a set of z chambers that measure the track coordinates along the beam direction.

A lead-glass electromagnetic calorimeter located outside the magnet coil covers the full azimuthal range with excellent hermeticity in the polar angle range of $|\cos\theta| < 0.82$ for the barrel region and $0.81 < |\cos\theta| < 0.984$ for the endcap region (EE). Electromagnetic calorimeters close to the beam axis complete the geometrical acceptance down to approximately 25 mrad. These include the forward detectors (FD) which are lead-scintillator sandwich calorimeters and, at smaller angles, silicon tungsten calorimeters (SW) located on both sides of the interaction point. The gap between the EE and FD calorimeters is instrumented with an additional lead-scintillator electromagnetic calorimeter, called the gamma-catcher (GC).

The magnet return yoke is instrumented for hadron calorimetry and consists of barrel and endcap sections along with pole tip detectors that together cover the region $|\cos\theta| < 0.99$. Outside the hadron calorimeter, four layers of muon chambers cover the polar angle range of $|\cos\theta| < 0.98$. Arrays of thin scintillating tiles with embedded wavelength shifting fibre readout have been installed in the endcap region to improve trigger performance, time resolution and hermeticity for experiments at LEP II [7]. Of particular relevance to this analysis are the four layers of scintillating tiles (the MIP plug) installed at each end of OPAL covering the angular range $43 < \theta(\text{mrad}) < 220$.

The following Standard Model processes are simulated at $\sqrt{s} = 183$ GeV. 4-fermion production is generated using grc4f [10], PYTHIA [11] and EXCALIBUR [12]. Two-photon processes are generated using the program of Vermaseren [13] and grc4f for $e^+e^-\ell^+\ell^-$, and using PHOJET [14], HERWIG [15] and grc4f for $e^+e^-q\overline{q}$. Because of the large total cross-section for $e^+e^-e^+e^-$, $e^+e^-\mu^+\mu^-$ and $e^+e^-q\overline{q}$, soft cuts are applied at the generator level to preselect events that might possibly lead to background in the selection of $\ell^+\nu\ell^-\overline{\nu}$ final states. No generator level cuts are applied to the $e^+e^-\tau^+\tau^-$ generation. The production of lepton pairs is generated using BHWIDE [16] and TEEGG [17] for $e^+e^-(\gamma)$, and using KORALZ [18] for $\mu^+\mu^-(\gamma)$, $\tau^+\tau^-(\gamma)$ and $\nu\overline{\nu}\gamma\gamma$. The production of quark pairs, $q\overline{q}(g)$, is generated using PYTHIA. The effective

5

Monte Carlo integrated luminosities exceed that of the data by factors that are typically of the order of one thousand and in all cases are at least twenty.

Slepton pair production is generated using SUSYGEN [19]. Charged Higgs boson pair production is generated using HZHA [20] and PYTHIA. Chargino pair production is generated using DFGT [21] and SUSYGEN.

All Standard Model and new physics Monte Carlo samples are processed with a full simulation of the OPAL detector [22] and subjected to the same reconstruction and analysis programs as used for the OPAL data.

3 General Selection of Di-lepton Events with Significant Missing Momentum

The general selection of di-lepton events with significant missing momentum is largely unchanged with respect to [1]. In selecting candidate events the missing momentum is required to have a significant component in the plane perpendicular to the beam axis (p_t^{miss}). This generally leads to an acoplanar[3] event topology. Standard Model background with high energy particles escaping down the beam pipe and giving rise to missing momentum along the beam axis is thus rejected. A potential background arises from lepton pairs produced in two-photon processes in which one of the initial state electrons is scattered at a significant angle to the beam direction. Such processes are suppressed by vetoing on energy being present in the forward region (SW, FD or GC calorimeters).

The OPAL detector provides hermetic coverage for electrons and photons for $\theta > 25$ mrad. However, prior to the data collection at $\sqrt{s} = 183$ GeV it was possible for a muon in the angular range $60 < \theta(\text{mrad}) < 160$ to escape detection. This led to a background to the general selection from $\text{e}^+\text{e}^-\mu^+\mu^-$ events in which one electron and one muon were observed in the detector. In order to improve the detection of muons in the forward region, four layers of scintillating tile detectors (the MIP plug) were installed at each end of OPAL. In the data at $\sqrt{s} = 183$ GeV the OPAL detector provides hermetic coverage for muons for $\theta > 25$ mrad.

A new selection cut is introduced to make use of the MIP plug detector. Candidate events are vetoed if they contain coincident hits in two or more scintillator layers in the MIP plug at the same ϕ and at the same end of OPAL, satisfying cuts on pulse height and timing. The efficiency to detect a muon within the geometrical acceptance of the MIP plug with these cuts is measured to be $80 \pm 4\%$ by using $\text{e}^+\text{e}^-\mu^+\mu^-$ events in which a minimum ionizing track is observed in SW within the MIP plug geometrical acceptance. Note that this efficiency includes the effect of periods when the MIP plug was not fully operational. The cut on MIP plug activity exclusively rejects three events in the data at $\sqrt{s} = 183$ GeV; this may be compared with the Standard Model expectation of 2.5 events, of which 2.3 arise from the $\text{e}^+\text{e}^-\mu^+\mu^-$ final state. In addition to the cut on MIP plug activity, minor changes to improve the rejection of two-photon processes and "junk" events arising from, e.g., beam-gas interactions have been made with respect to the selection cuts described in [1].

The numbers of events passing the general selection at each centre-of-mass energy in the data are compared to the Standard Model Monte Carlo predictions in table 1. The total

---

[3]The acoplanarity angle is defined as 180° minus the angle between the two lepton candidates in the plane transverse to the beam direction.

$\sqrt{s}$ (GeV)	data	SM	$\ell^+\nu\,\ell^-\overline{\nu}$	$\mathrm{e^+e^-}\ell^+\ell^-$	$\mathrm{e^+e^-}\,\mathrm{q\overline{q}}$	$\ell^+\ell^-(\gamma)$
161	4	4.5±0.3	3.4±0.1	0.9±0.2	0.1±0.1	0.1±0.0
172	9	11.6±0.3	10.7±0.1	0.8±0.2	0.0±0.0	0.1±0.0
183	78	81.3±0.7	77.6±0.7	3.2±0.0	0.0±0.0	0.5±0.2

Table 1: *Comparison between data and Monte Carlo of the number of events passing the general selection at each centre-of-mass energy. The total number of events predicted by the Standard Model is given, together with a breakdown into the contributions from individual processes. At each centre-of-mass energy the Standard Model Monte Carlos are normalised to an integrated luminosity that corresponds to the collected experimental luminosity. The Monte Carlo statistical errors are given.*

Lepton identification	data	SM
$\mathrm{e^+e^-}$	14	12.3
$\mu^+\mu^-$	13	13.6
$h^\pm h^\mp$	1	2.3
$\mathrm{e^\pm}\mu^\mp$	20	25.6
$\mathrm{e^\pm h^\mp}$	8	9.8
$\mu^\pm h^\mp$	8	9.3
$\mathrm{e^\pm}$, unidentified	5	3.8
$\mu^\pm$, unidentified	7	3.7
$h^\pm$, unidentified	2	0.9

Table 2: *The lepton identification information in the events passing the general selection compared with the Standard Model Monte Carlo at $\sqrt{s} = 183$ GeV. "h" means that the lepton is identified neither as an electron nor muon and so is probably the product of a hadronic tau decay. Leptonic decays of taus are usually classified as electron or muon. "Unidentified" means that only one isolated lepton has been positively identified in the event. (For details see the description of cut 3 in Appendix I.3 of [1].)*

number of events predicted by the Standard Model is given, together with a breakdown into the contributions from individual processes. The number of observed candidates is consistent with the expectation from Standard Model sources, which is dominated by the $\ell^+\nu\,\ell^-\overline{\nu}$ final state arising from $\mathrm{W^+W^-}$ production in which both W's decay leptonically: $\mathrm{W^-} \to \ell^-\overline{\nu}_\ell$.

The second stage event selection to distinguish between Standard Model and new physics sources of lepton pair events with missing momentum is described in section 4. Discrimination is provided by information on the lepton identification, and the energy and $-q\cos\theta$ of the observed lepton candidates, where q is the lepton charge. We check here on the degree to which these quantities are described by the Standard Model Monte Carlo. The lepton identification information in the event sample produced by the general selection at $\sqrt{s} = 183$ GeV is compared with the Standard Model Monte Carlo in table 2. For the same event sample, figure 1 shows the distributions of (a) the energy scaled by the beam energy and (b) the value of $-q\cos\theta$ of each charged lepton candidate. The data, shown as points with error bars, are compared with the Standard Model Monte Carlo predictions, which are dominated by the final state $\ell^+\nu\,\ell^-\overline{\nu}$.

Figure 2 (a) shows the distribution of $p_t^{\mathrm{miss}}/E_{\mathrm{beam}}$ for the general selection at $\sqrt{s} = 183$ GeV. As a test of the degree to which the Standard Model Monte Carlo describes the $\mathrm{e^+e^-}\ell^+\ell^-$ background, figure 2 (b) shows the distribution of $p_t^{\mathrm{miss}}/E_{\mathrm{beam}}$ after we relax some of the event selection cuts, as described in appendix I.3 of [1]. With these relaxed cuts the number of observed candidates at $\sqrt{s} = 183$ GeV is 145; this is consistent with the 149.3 ± 2.0 events expected from Standard Model sources, of which 66.3 ± 1.9 arise from the final state $\mathrm{e^+e^-}\ell^+\ell^-$. In each of the above checks the data are consistent with the Standard Model expectations.

The cuts used to veto two-photon background introduce an inefficiency in the event selection due to random detector occupancy (principally in the SW, FD and MIP plug detectors) that is not modelled in the Monte Carlo. This inefficiency has been measured using randomly triggered events collected during normal data taking. In the data collected at $\sqrt{s} = 183$ GeV the inefficiency decreases from a value of 8.2% for events with very low missing transverse momentum to a negligible value for events with $p_t^{\mathrm{miss}}/E_{\mathrm{beam}} > 0.25$. At $\sqrt{s} = 161$ and 172 GeV the backgrounds from off-momentum electrons in LEP were much lower and the veto inefficiency was around 3% for events with very low missing transverse momentum. When quoting expected numbers of Standard Model events and selection efficiencies for potential new physics sources, the variation of veto inefficiency with p_t^{miss} is taken into account.

4   Additional Selection Criteria for New Particle Searches

Starting from the general selection of events containing two charged leptons and missing transverse momentum that was discussed in section 3, we search for the production of new particles by applying additional cuts to suppress Standard Model sources of such events, the most important of which are $\ell^+\nu\,\ell^-\overline{\nu}$ and $\mathrm{e^+e^-}\ell^+\ell^-$.

The Standard Model $\ell^+\nu\,\ell^-\overline{\nu}$ events from $\mathrm{W^+W^-}$ are characterised by the production of two leptons, both with p/E_{beam} around 0.5. Equal numbers of $\mathrm{e}^\pm$, $\mu^\pm$ and $\tau^\pm$ are produced and there is no correlation between the flavours of the two charged leptons in the event. In the Standard Model $\mathrm{e^+e^-}\ell^+\ell^-$ events the two observed leptons tend to have low momentum.

In the signal events the momentum distribution of the expected leptons varies strongly as a function of the mass difference, Δm between the parent particle (e.g., selectron) and the invisible daughter particle (e.g., lightest neutralino), and, to a lesser extent, m, the mass of the parent particle. Slepton and charged Higgs boson pairs decay to produce two charged leptons of the same flavour. When performing a search for a particular new particle at a particular point in m and Δm, an event is considered as a potential candidate only if the properties of the observed leptons are consistent with expectations for signal events at those values of m and Δm.

The method employed here differs from that described in [1] in two respects:

1. Use of the $-q\cos\theta$ of the two lepton candidates to discriminate against the Standard Model background in addition to the information on the lepton identification and energy of the lepton candidates.

2. Use of a likelihood technique to combine information from the various discriminating variables.

8

As is demonstrated by figure 1 (b), the distribution of $-q\cos\theta$ of the lepton candidates in W^+W^- events is strongly forward peaked. This may be compared with the dashed histogram in figure 1 (b), which corresponds to the distribution expected from smuon pair production and decay. The distribution for smuons is symmetric about $\cos\theta = 0$. This is because the smuon is a scalar; the angular distribution for s-channel production of smuon pairs is expected to be proportional to $\sin^2\theta$ and the decay muon is expected to be isotropic in the smuon rest frame. In the search for pair production of smuons, staus and charged Higgs bosons the value of $-q\cos\theta$ of the two lepton candidates is used to discriminate against the Standard Model background in addition to the information on the lepton identification and energy of the lepton candidates.

Selectrons may be produced via t-channel neutralino exchange in addition to s-channel production. This results in the expected $-q\cos\theta$ distribution of selectrons being model-dependent. Choices of model parameters are possible for which the t-channel exchange is dominant. In this case the distribution will be forward-peaked similar to that of the W^+W^- background. Similarly, charginos may be produced via t-channel sneutrino exchange. Therefore, the variable $-q\cos\theta$ is not used in the discrimination of signal and Standard Model background in the searches for selectrons and charginos.

Discrimination between Standard Model and new physics sources of lepton pair events with missing momentum is performed by considering the likelihood that an event is consistent with being either signal or background. Given an event, for which the values of a set of variables x_i are known, the likelihood[4], L_S, of the event being consistent with the signal hypothesis is calculated as the product of the probabilities $P(x_i, S)$ that the signal hypothesis would produce an event with variable i having value x_i:

$$L_S = \prod_i P(x_i, S).$$

The likelihood, L_B, of an event being consistent with the background hypothesis is calculated similarly. The quantity L_R is defined by:

$$L_R = \frac{L_S}{L_S + L_B}.$$

Event selection is performed by making a cut on the value of L_R rather than on the individual variables x_i, which was the method used in [1]. Distributions of L_R for data and Standard Model Monte Carlo are compared for example values of m and Δm at $\sqrt{s} = 183$ GeV, for selectrons, smuons and staus in figure 3.

The optimisation of the selection cuts proceeds in a way similar to that described in [1]: the *a priori* average value of the 95% CL upper limit on the cross-section for new physics is minimised by means of an automated procedure that makes use of Monte Carlo samples of signal and Standard Model backgrounds, but not the experimental data. The optimisation is performed separately at each centre-of-mass energy.

---

[4]Because the variables x_i are correlated to some degree, L_S is only an approximation to the true likelihood. However, since the signal efficiencies and expected Standard Model backgrounds are estimated by applying the derived cuts to Monte Carlo samples no error is introduced into the quoted results.

5 Numbers of Candidates, Backgrounds and Efficiencies

At example points in m and Δm, table 3 gives the number of selected events, the number of events expected from Standard Model processes and the selection efficiency for new physics, of the searches at $\sqrt{s} = 183$ GeV for $\tilde{e}^+\tilde{e}^-$, $\tilde{\mu}^+\tilde{\mu}^-$ and $\tilde{\tau}^+\tilde{\tau}^-$. Table 4 gives the same information for the searches for $\tilde{\chi}_1^+\tilde{\chi}_1^-$ (2-body decays: $\tilde{\chi}_1^\pm \to \ell^\pm\tilde{\nu}_\ell$) and $\tilde{\chi}_1^+\tilde{\chi}_1^-$ (3-body decays: $\tilde{\chi}_1^\pm \to W^\pm\tilde{\chi}_1^0 \to \ell^\pm\nu\tilde{\chi}_1^0$). The Monte Carlo statistical errors are given.

It should be noted that an individual candidate event may be consistent with a given new physics hypothesis over a range of m and Δm values. Similarly, an individual candidate event may be consistent with more than one new physics hypothesis and may, therefore, give entries in more than one of the above tables. At high Δm, the expected number of Standard Model events is made up almost entirely (typically greater than 98%) of W^+W^- events, whereas at low Δm, it is typical for approximately half of the Standard Model events to arise from W^+W^- events, with the remainder arising predominantly from two-photon events.

For each search channel, table 5 shows the total number of selected candidates over all values of m and Δm compared with the Standard Model expectations.

In general, the Standard Model Monte Carlo provides a good description of the data in tables 3–5. The most significant difference between data and Monte Carlo is seen in table 3 for smuons at large Δm. The excess is most marked at $m = 65$ GeV, $\Delta m = m/2$. It is difficult to assess quantitatively the significance of this excess, given that there are strong correlations in the selected event samples: a) among individual bins for a particular search channel and b) among the six different search channels.

Slepton pair efficiencies are evaluated for right-handed sleptons, both decaying to lepton and lightest neutralino $\tilde{\ell}^\pm \to \ell^\pm\tilde{\chi}_1^0$. The slepton pair events were generated at $\mu = -200$ GeV and $\tan\beta = 1.5$ using SUSYGEN. The selection efficiency for selectrons depends on the angular distribution of the produced selectrons and this will depend on the size of the neutralino-mediated t-channel contribution to the cross-section. We have found by varying μ and $\tan\beta$ that the above choice gives a conservative estimate of the selection efficiency. In the generation of the stau pair events using SUSYGEN the produced taus are unpolarized. As noted in [23] the polarisation of taus in the decay of staus can vary from $+1$ to -1 depending on the neutralino field content. This leads to a model dependence of the expected momentum spectrum of the visible tau decay products.

The experimental signature of H^+H^- production followed by the decay $H^\pm \to \tau^\pm\nu_\tau$ is similar to that of $\tilde{\tau}^+\tilde{\tau}^-$ production, $\tilde{\tau}^+\tilde{\tau}^- \to \tau^+\tilde{\chi}_1^0\tau^-\tilde{\chi}_1^0$, for the case when the $\tilde{\chi}_1^0$ is massless and stable. The selection efficiencies for H^+H^- events generated using HZHA and PYTHIA are consistent with those for $\tilde{\tau}^+\tilde{\tau}^-$ events with $m_{\tilde{\chi}_1^0} = 0$ generated using SUSYGEN[5]. Because the available Monte Carlo samples for the latter process have higher statistics, we use them to evaluate the selection efficiencies for H^+H^-.

Monte Carlo samples for $\tilde{\chi}_1^+\tilde{\chi}_1^-$ production followed by the decay: $\tilde{\chi}_1^\pm \to \ell^\pm\tilde{\nu}$ (2-body decay) are generated using SUSYGEN. Given the limit of 37.1 GeV on the mass of the lightest sneutrino from LEP1 [24], $\tilde{\chi}_1^+\tilde{\chi}_1^-$ (2-body decays) events are not generated for sneutrino masses less than

---

[5]Note that in HZHA the tau polarisation in the decay $H^+ \to \tau^+\nu_\tau$ is handled correctly, whereas in SUSYGEN the taus are unpolarised. The average selection efficiencies obtained with the two Monte Carlos are consistent within the 3% statistical accuracy of the comparison. This represents a check of the model dependence also of the $\tilde{\tau}^+\tilde{\tau}^-$ selection efficiencies at high Δm.

Δm (GeV)	selectrons $m_{\tilde{e}^-}$ (GeV)			smuons $m_{\tilde{\mu}^-}$ (GeV)			staus $m_{\tilde{\tau}^-}$ (GeV)		
	65	80	90	65	80	90	65	80	90
number of selected events									
2	0	0	0	0	0	0	0	0	0
2.5	0	0	0	0	0	0	0	0	0
5	1	0	0	0	0	0	1	1	1
10	1	0	0	0	0	0	1	2	1
20	0	0	0	2	0	0	3	1	1
$m/2$	7	6	3	10	6	3	4	2	2
$m-20$	15	11	4	9	9	6	4	4	3
$m-10$	15	13	2	7	9	6	5	8	4
m	15	14	2	4	9	6	5	9	4
number of events expected from Standard Model processes									
2	0.5±0.1	0.3±0.1	0.1±0.1	0.1±0.1	0.0±0.0	0.0±0.0	0.1±0.1	0.1±0.1	0.1±0.1
2.5	0.5±0.1	0.3±0.1	0.2±0.1	0.2±0.1	0.1±0.1	0.0±0.0	0.6±0.2	0.3±0.1	0.1±0.1
5	0.6±0.2	0.5±0.2	0.1±0.1	0.3±0.1	0.1±0.1	0.1±0.1	1.8±0.3	1.4±0.2	1.1±0.2
10	0.4±0.1	0.1±0.1	0.0±0.0	0.4±0.1	0.2±0.1	0.0±0.0	2.6±0.3	2.2±0.3	2.0±0.3
20	1.7±0.1	0.4±0.0	0.1±0.0	1.8±0.1	0.6±0.1	0.1±0.0	3.9±0.3	2.1±0.2	1.8±0.2
$m/2$	5.3±0.2	3.5±0.1	0.9±0.1	3.9±0.2	3.7±0.2	1.3±0.1	5.8±0.3	6.0±0.3	5.1±0.3
$m-20$	10.8±0.2	7.7±0.2	1.5±0.1	4.6±0.2	5.2±0.2	1.7±0.1	7.3±0.3	9.1±0.4	6.7±0.3
$m-10$	10.9±0.2	9.2±0.2	1.6±0.1	4.0±0.2	5.2±0.2	1.8±0.1	7.7±0.3	9.6±0.4	6.1±0.3
m	11.1±0.2	9.5±0.2	1.8±0.1	3.0±0.1	5.6±0.2	2.2±0.1	7.6±0.3	10.1±0.4	6.6±0.3
selection efficiency (%)									
2	8±1	3±1	1±0	10±1	2±0	0±0	0±0	0±0	0±0
2.5	24±1	18±1	12±1	24±1	15±1	11±1	0±0	0±0	0±0
5	51±2	53±2	54±2	56±2	55±2	57±2	10±0	8±0	8±0
10	64±1	60±1	64±1	67±1	70±1	71±1	25±1	25±1	24±1
20	65±1	69±1	69±1	70±1	76±1	76±1	36±1	34±1	33±1
$m/2$	63±1	66±1	68±1	63±1	70±1	75±1	41±1	46±1	48±1
$m-20$	70±1	69±1	67±1	63±1	68±1	68±1	44±1	51±1	47±1
$m-10$	72±1	74±1	64±1	61±1	67±1	66±1	43±1	51±1	44±1
m	73±1	74±1	67±1	55±1	68±1	71±1	43±1	52±1	45±1

Table 3: *Search for slepton pairs at $\sqrt{s} = 183$ GeV. The number of selected events, the number of events expected from Standard Model processes and the selection efficiency for different values of $m_{\tilde{\ell}}$ and Δm. The selection efficiency for $\tilde{\tau}^+ \tilde{\tau}^-$ is calculated for the case that the decay $\tilde{\tau}^- \to \tau^- \tilde{\chi}_1^0$ produces unpolarized $\tau^{\pm}$.*

$\tilde{\chi}_1^+\tilde{\chi}_1^-$ (2-body decays)				$\tilde{\chi}_1^+\tilde{\chi}_1^-$ (3-body decays)			
Δm	$m_{\tilde{\chi}_1^\pm}$ (GeV)			Δm	$m_{\tilde{\chi}_1^\pm}$ (GeV)		
(GeV)	65	80	90	(GeV)	65	80	90
number of selected events							
1.5	1	0	0	3	0	0	0
2.5	0	0	0	5	0	0	0
5	2	0	0	10	2	2	1
10	3	1	1	20	3	3	2
20	5	2	1	$m/2$	3	3	1
$(m-15)/2$	13	16	4	$m-20$	5	5	11
$m-35$	37	43	29	$m-10$	11	22	19
				m	51	54	27
number of events expected from Standard Model processes							
1.5	1.5±0.2	0.1±0.1	0.1±0.1	3	0.6±0.1	0.5±0.1	0.6±0.2
2.5	1.1±0.2	0.8±0.2	0.2±0.1	5	1.5±0.2	0.8±0.2	0.7±0.2
5	2.7±0.3	1.2±0.2	0.6±0.2	10	4.1±0.4	2.5±0.3	1.6±0.2
10	5.1±0.4	1.6±0.2	0.7±0.1	20	7.0±0.5	4.7±0.4	2.3±0.3
20	14.7±0.5	4.3±0.3	1.4±0.2	$m/2$	9.9±0.5	6.3±0.4	4.5±0.3
$(m-15)/2$	22.1±0.5	20.5±0.5	9.3±0.3	$m-20$	13.4±0.5	14.9±0.5	17.7±0.5
$m-35$	42.5±0.6	51.4±0.7	33.9±0.6	$m-10$	21.5±0.6	27.7±0.6	25.7±0.5
				m	53.5±0.7	60.2±0.7	30.4±0.5
selection efficiency (%)							
1.5	0±0	0±0	0±0	3	3±0	1±0	1±1
2.5	14±1	7±0	5±1	5	15±1	13±1	10±1
5	45±2	34±1	39±1	10	39±1	38±1	38±1
10	54±2	44±2	45±2	20	48±2	49±2	45±2
20	60±1	62±1	58±2	$m/2$	51±2	51±2	53±2
$(m-15)/2$	—	67±1	67±1	$m-20$	51±2	54±2	65±1
$m-35$	65±1	73±1	70±1	$m-10$	53±2	61±1	64±1
				m	67±1	74±1	71±1

Table 4: *Search for chargino pairs (2-body decays: $\tilde{\chi}_1^\pm \to \ell^\pm \tilde{\nu}_\ell$ and 3-body decays: $\tilde{\chi}_1^\pm \to W^\pm \tilde{\chi}_1^0 \to \ell^\pm \nu \tilde{\chi}_1^0$) at $\sqrt{s} = 183$ GeV. The number of selected events, the number of events expected from Standard Model processes and the selection efficiency for different values of $m_{\tilde{\chi}_1^\pm}$ and Δm.*

Search	$\sqrt{s}$ (GeV)					
Channel	161		172		183	
	data	SM	data	SM	data	SM
$\tilde{e}^+\tilde{e}^-$	1	1.0	2	2.2	16	14.0
$\tilde{\mu}^+\tilde{\mu}^-$	1	0.8	2	2.0	13	11.5
$\tilde{\tau}^+\tilde{\tau}^-$	2	1.4	4	2.9	11	13.0
H^+H^-	1	1.0	4	2.6	9	11.5
$\tilde{\chi}_1^+\tilde{\chi}_1^-$ (3-body decays)	3	3.3	7	8.4	62	71.0
$\tilde{\chi}_1^+\tilde{\chi}_1^-$ (2-body decays)	2	2.9	7	7.3	48	58.2

Table 5: *For each search channel at each value of $\sqrt{s}$, the total number of selected candidates over all values of m and Δm compared with the Standard Model expectations.*

35 GeV. Monte Carlo samples for $\tilde{\chi}_1^+\tilde{\chi}_1^-$ production in which the chargino decays via a virtual or real W, $\tilde{\chi}_1^\pm \to W^\pm \tilde{\chi}_1^0 \to \ell^\pm \nu \tilde{\chi}_1^0$, (3-body decays) are generated using DFGT at $\sqrt{s} = 183$ GeV and SUSYGEN at $\sqrt{s} = 161$ and 172 GeV.

It can be seen that sizable selection efficiencies have been obtained for $\tilde{e}^+\tilde{e}^-$, $\tilde{\mu}^+\tilde{\mu}^-$ and $\tilde{\chi}_1^+\tilde{\chi}_1^-$ (2-body decays), even when Δm is as low as 2 GeV. However, for $\tilde{\tau}^+\tilde{\tau}^-$ and $\tilde{\chi}_1^+\tilde{\chi}_1^-$ (3-body decays) there are additional invisible particles (neutrinos) in the final state. The visible leptons are therefore less energetic and the selection efficiencies at low Δm values are reduced.

6 New Particle Search Results

The number of observed candidate events and their kinematic properties are compatible with the expectations from Standard Model processes. We present limits on the pair production of charged scalar leptons, leptonically decaying charged Higgs bosons and charginos that decay to produce a charged lepton and invisible particles. The sensitivity of the searches is significantly improved with respect to [1] because of: the increased centre-of-mass energy and integrated luminosity; the reduced $e^+e^-\ell^+\ell^-$ background achieved due to the detector upgrade (MIP plug); and the improved analysis techniques (use of $-q\cos\theta$ and likelihood techniques).

As described in section 4, the additional event selection cuts for a given search channel vary as a function of m and Δm. As input to the limit calculation for each new particle search we calculate at each value of m, Δm, and $\sqrt{s}$: the number of observed candidates, the number of expected events from Standard Model background, the selection efficiency, and the pair production cross-section relative to that at $\sqrt{s} = 183$ GeV. The 95% CL upper limits at $\sqrt{s} = 183$ GeV are obtained by combining the data at the three e^+e^- centre-of-mass energies 161, 172 and 183 GeV using the Likelihood Ratio method [8].

The number of selected candidate events is determined at each kinematically allowed point on a 0.2 GeV by 0.2 GeV grid of m and Δm. Monte Carlo signal events are available only at certain particular values of m and Δm. The values of m range typically from $m = 45$ GeV up to $m \approx E_{\text{beam}}$ in 5 GeV steps. The values of Δm correspond to those given in tables 3 and 4. Signal efficiencies at intermediate values of m and Δm are obtained by linear 2-dimensional interpolation. In addition to the Monte Carlo statistical error, we assign a 5% systematic error on the estimated selection efficiency to take into account uncertainties in: trigger efficiency,

detector occupancy, lepton identification efficiency, luminosity measurement, interpolation procedure, and deficiencies in the Monte Carlo generators and the detector simulation.

At high values of Δm the dominant background to the searches for new physics results from W^+W^- production. High statistics Monte Carlo samples for this process are available that describe well the OPAL data [2, 3, 4]. In addition to the Monte Carlo statistical error, we assign a 5% systematic error on the estimated background to take into account deficiencies in the Monte Carlo detector simulation. At low values of Δm the dominant background results from $e^+e^-\ell^+\ell^-$ events. The background uncertainty at low Δm is dominated by the limited Monte Carlo statistics; the uncertainty is typically 20–80% at low Δm. In setting limits the Monte Carlo statistical errors and other systematics are taken into account according to the method described in [25].

Limits on the production cross-section times branching ratio squared for new physics processes are now presented in a manner intended to minimise the number of model assumptions. The 95% CL upper limits at $\sqrt{s} = 183$ GeV shown in figures 4 – 8 are obtained by combining the data at the three e^+e^- centre-of-mass energies 161, 172 and 183 GeV using the assumption that the cross-section varies as β^3/s for sleptons and β/s for charginos. The chosen functional forms are used for simplicity in presenting the data and represent an approximation, particularly for processes in which t-channel exchange may be important, that is, selectron pair and chargino pair production. In these cases the cross-section dependence on e^+e^- centre-of-mass energy is model dependent, depending on the mass of the exchanged particles and the couplings of the neutralinos and charginos.

Upper limits at 95% CL on the selectron pair cross-section at $\sqrt{s} = 183$ GeV times branching ratio squared for the decay $\tilde{e}^- \to e^-\tilde{\chi}_1^0$ are shown in figure 4 as a function of selectron mass and lightest neutralino mass. These limits are applicable to $\tilde{e}_L^+\tilde{e}_L^-$ and $\tilde{e}_R^+\tilde{e}_R^-$ production. The corresponding plots for the smuon and stau pair searches are shown in figures 5 and 6, respectively. Note that if the LSP is the gravitino (effectively massless), then for prompt slepton decays to lepton-gravitino the experimental signature would be the same as that for $\tilde{\ell}^- \to \ell^-\tilde{\chi}_1^0$ with a massless neutralino. In this case the limits given in figures 4 – 6 for $m_{\tilde{\chi}_1^0} = 0$ may be interpreted as limits on the decay to lepton-gravitino.

The upper limit at 95% CL on the chargino pair production cross-section times branching ratio squared for the decay $\tilde{\chi}_1^\pm \to \ell^\pm \tilde{\nu}_\ell$ (2-body decay) is shown in figure 7. The limit has been calculated for the case where the three sneutrino generations are mass degenerate. The upper limit at 95% CL on the chargino pair production cross-section times branching ratio squared for the decay $\tilde{\chi}_1^\pm \to W^\pm \tilde{\chi}_1^0 \to \ell^\pm \nu \tilde{\chi}_1^0$ (3-body decay) is shown in figure 8. In a forthcoming paper [26] the search described here for acoplanar di-lepton events will be combined with searches in other final states to set more general limits on chargino pair production.

The upper limit at 95% CL on the charged Higgs boson pair production cross-section times branching ratio squared for the decay $H^+ \to \tau^+\nu_\tau$ is shown as a function of m_{H^+} as the solid line in figure 9. The limit is obtained by combining the 161–183 GeV data-sets assuming the m_{H^+} and $\sqrt{s}$ dependence of the cross-section predicted by PYTHIA, which takes into account the effect of initial state radiation. The dashed line in figure 9 shows the prediction from PYTHIA at $\sqrt{s} = 183$ GeV for a 100% branching ratio for the decay $H^+ \to \tau^+\nu_\tau$. With this assumption we set a lower limit at 95% CL on m_{H^+} of 73 GeV. In a forthcoming paper [27] the search described here for acoplanar di-tau events will be combined with searches in the final states $\tau\overline{\nu}q\overline{q}$ and $q\overline{q}q\overline{q}$ to set limits on charged Higgs boson pair production for arbitrary $H^+ \to \tau^+\nu_\tau$ branching ratio.

We can use our data to set limits on the masses of right-handed sleptons[6] based on the expected right-handed slepton pair cross-sections and branching ratios. The cross-sections have been calculated using SUSYGEN at each centre-of-mass energy and take into account initial state radiation. In figure 10 we show limits on right-handed smuons as a function of smuon mass and lightest neutralino mass for several assumed values of the branching ratio squared for $\tilde{\mu}_R^\pm \to \mu^\pm \tilde{\chi}_1^0$. The expected limit, calculated using Monte Carlo only, for a branching ratio of 100% is also shown. Note that the actual limit is lower than expected for large Δm as a result of the excess of events seen for smuons at $\sqrt{s} = 183$ GeV. For a branching ratio $\tilde{\mu}_R^\pm \to \mu^\pm \tilde{\chi}_1^0$ of 100% and for a smuon-neutralino mass difference exceeding 2 GeV, right-handed smuons are excluded at 95% CL for masses below 65 GeV. The 95% CL upper limit on the production of right-handed $\tilde{\tau}^+ \tilde{\tau}^-$ times the branching ratio squared for $\tilde{\tau}_R^\pm \to \tau^\pm \tilde{\chi}_1^0$ is shown in figure 11. The expected limit for a branching ratio of 100% is also shown. For a branching ratio $\tilde{\tau}_R^\pm \to \tau^\pm \tilde{\chi}_1^0$ of 100% and for a stau-neutralino mass difference exceeding 10 GeV, right-handed staus are excluded at 95% CL for masses below 64 GeV. For the case of a massless neutralino (or gravitino) and 100% branching ratio, right-handed smuons and staus are excluded at 95% CL for masses below 68 GeV and 70 GeV, respectively.

An alternative approach is to set limits taking into account the predicted cross-section and branching ratio for specific choices of the parameters within the Minimal Supersymmetric Standard Model (MSSM)[7]. For $\mu < -100$ GeV and for two values of $\tan \beta$ (1.5 and 35), figures 12, 13 and 14 show 95% CL exclusion regions in the $(m_{\tilde{\ell}_R^\pm}, m_{\tilde{\chi}_1^0})$ plane for right-handed selectrons, smuons and staus, respectively. For $\mu < -100$ GeV and $\tan \beta = 1.5$, right-handed sleptons are excluded at 95% CL as follows: selectrons with masses below 77 GeV for $m_{\tilde{e}^-} - m_{\tilde{\chi}_1^0} > 5$ GeV; smuons with masses below 65 GeV for $m_{\tilde{\mu}^-} - m_{\tilde{\chi}_1^0} > 2$ GeV; and staus with masses below 60 GeV for $m_{\tilde{\tau}^-} - m_{\tilde{\chi}_1^0} > 9$ GeV.

7 Summary and Conclusions

A selection of di-lepton events with significant missing transverse momentum is performed using a total data sample of 77.0 pb^{-1} at e$^+$e$^-$ centre-of-mass energies of 161, 172 and 183 GeV. The observed numbers of events, four at 161 GeV, nine at 172 GeV and 78 at 183 GeV, are consistent with the numbers expected from Standard Model processes, dominantly arising from W$^+$W$^-$ production with each W decaying leptonically.

Further event selection criteria are employed to search for the pair production of charged scalar leptons, leptonically decaying charged Higgs bosons and charginos that decay to produce a charged lepton and one or more invisible particles. The sensitivity to new physics is maximised by using an algorithm to optimise the cut values as functions of the masses of the pair produced new particle and the unobserved particle produced in its decay. No evidence for new phenomena is apparent and model independent limits on the production cross-section times branching ratio squared for each new physics process are presented.

---

[6]The right-handed slepton is expected to be lighter than the left-handed slepton. The right-handed one tends (not generally valid for selectrons) to have a lower pair production cross-section, and so conventionally limits are given for this (usually) conservative case.

[7]In particular regions of the MSSM parameter space, the branching ratio for $\tilde{\ell}^\pm \to \ell^\pm \tilde{\chi}_1^0$ can be essentially zero and so it is not possible to provide general limits on sleptons within the MSSM on the basis of this search alone. The predicted cross-sections and branching ratios within the MSSM are obtained using SUSYGEN and are calculated with the gauge unification relation, $M_1 = \frac{5}{3} \tan^2 \theta_W M_2$.

Assuming a 100% branching ratio for the decay $\tilde{\ell}_R^\pm \to \ell^\pm \tilde{\chi}_1^0$, we exclude at 95% CL: right-handed smuons with masses below 65 GeV for $m_{\tilde{\mu}^-} - m_{\tilde{\chi}_1^0} > 2$ GeV and right-handed staus with masses below 64 GeV for $m_{\tilde{\tau}^-} - m_{\tilde{\chi}_1^0} > 10$ GeV. Right-handed selectrons are excluded at 95% CL for masses below 77 GeV for $m_{\tilde{e}^-} - m_{\tilde{\chi}_1^0} > 5$ GeV within the framework of the MSSM assuming $\mu < -100$ GeV and $\tan\beta = 1.5$.

Acknowledgements.

References

[1] OPAL Collaboration, K. Ackerstaff *et al.*, Eur. Phys. J. **C4** (1998) 47.

[2] OPAL Collaboration, K. Ackerstaff *et al.*, Phys. Lett. **B389** (1996) 416.

[3] OPAL Collaboration, K. Ackerstaff *et al.*, Eur. Phys. J. **C1** (1998) 395.

[4] OPAL Collaboration, *"Measurement of the* W^+W^- *Production Cross Section and Triple Gauge Boson Couplings at LEP"*, paper in preparation.

[5] H. P. Nilles, Phys. Rep. **110** (1984) 1;
H. E. Haber and G. L. Kane, Phys. Rep. **117** (1985).

[6] ALEPH Collaboration, R. Barate *et al.*, *" Search for Sleptons in* e^+e^- *Collisions at Centre-Of-Mass Energies up to 184 GeV"*, CERN-EP/98-077 (Submitted to Phys. Lett. B).
L3 Collaboration, M. Acciarri *et al.*, Eur. Phys. J. **C4** (1998) 207.

[7] G. Aguillion *et al.*, *"Thin Scintillating Tiles with High Light Yield for the OPAL Endcaps"*, CERN-EP/98-069 (accepted for publication by Nucl. Instrum. Methods).

[8] A.G. Frodesen, O. Skeggestad, and H. Tofte, *"Probability and Statistics in Particle Physics"*, Universitetsforlaget, 1979, ISBN 82-00-01-01906-3;
S.L. Meyer, *"Data Analysis for Scientists and Engineers"*, John Wiley and Sons, 1975, ISBN 0-471-59995-6.

[9] OPAL Collaboration, K. Ahmet *et al.*, Nucl. Instrum. Methods **A305** (1991) 275;
S. Anderson *et al.*, Nucl. Instrum. Methods **A403** (1998) 326;
B. E. Anderson *et al.*, IEEE. Trans. Nucl. Sci. **41** (1994) 845.

[10] grc4f 1.0 generator: J. Fujimoto *et al.*, Comp. Phys. Comm. **100** (1997) 128;
J. Fujimoto *et al.*, in *"Physics at LEP2"*, edited by G. Altarelli, T. Sjöstrand and F. Zwirner, CERN 96-01, vol. 2 (1996) p. 30.

[11] PYTHIA 5.721 and JETSET 7.408 generators: T. Sjöstrand, Comp. Phys. Comm. **82** (1994) 74; LU TP 95-20.

[12] EXCALIBUR generator: F.A. Berends, R. Pittau, R. Kleiss, Comp. Phys. Comm. **85** (1995) 437.

[13] J. A. M. Vermaseren, Nucl. Phys. **B229** (1983) 347.

[14] PHOJET 1.05 generator: E. Budinov *et al.*, in *"Physics at LEP2"*, edited by G. Altarelli, T. Sjöstrand and F. Zwirner, CERN 96-01, vol. 2 (1996) p. 216;
R. Engel and J. Ranft, Phys. Rev. **D54** (1996) 4244.

[15] G. Marchesini *et al.*, Comp. Phys. Comm. **67** (1992) 465.

[16] BHWIDE generator: S. Jadach, W. Płaczek, B. F. L. Ward, Phys. Lett. **390** (1997) 298.

[17] TEEGG generator: D. Karlen, Nucl. Phys. **B289** (1987) 23.

[18] KORALZ 4.0 generator: S. Jadach, B. F. L. Ward, Z. Wąs, Comp. Phys. Comm. **79** (1994) 503.

[19] SUSYGEN generator: S. Katsanevas and S. Melachroinos, in *"Physics at LEP2"*, edited by G. Altarelli, T. Sjöstrand and F. Zwirner, CERN 96-01, vol. 2 (1996) p. 216.

[20] HZHA generator: P. Janot, in *"Physics at LEP2"*, edited by G. Altarelli, T. Sjöstrand and F. Zwirner, CERN 96-01, vol. 2 (1996) p. 309.

[21] DFGT generator: C. Dionisi *et al.*, in *"Physics at LEP2"*, edited by G. Altarelli, T. Sjöstrand and F. Zwirner, CERN 96-01, vol.2 (1996) p. 337.

[22] J. Allison *et al.*, Nucl. Instrum. Methods **A317** (1992) 47.

[23] M. Nojiri, Phys. Rev. **D51** (1995) 6281.

[24] L3 Collaboration, O. Adriani *et al.*, Phys. Rep. **236** (1993) 1.

[25] R. D. Cousins and V. L. Highland, Nucl. Instrum. Methods **A320** (1992) 331.

[26] OPAL Collaboration, *"Search for Chargino and Neutralino Production in e^+e^- Collisions at $\sqrt{s} = 181 - 184\ GeV$"*, paper in preparation.

[27] OPAL Collaboration, *"Search for Higgs bosons in e^+e^- collisions at $\sqrt{s} = 183\ GeV$"*, paper in preparation.
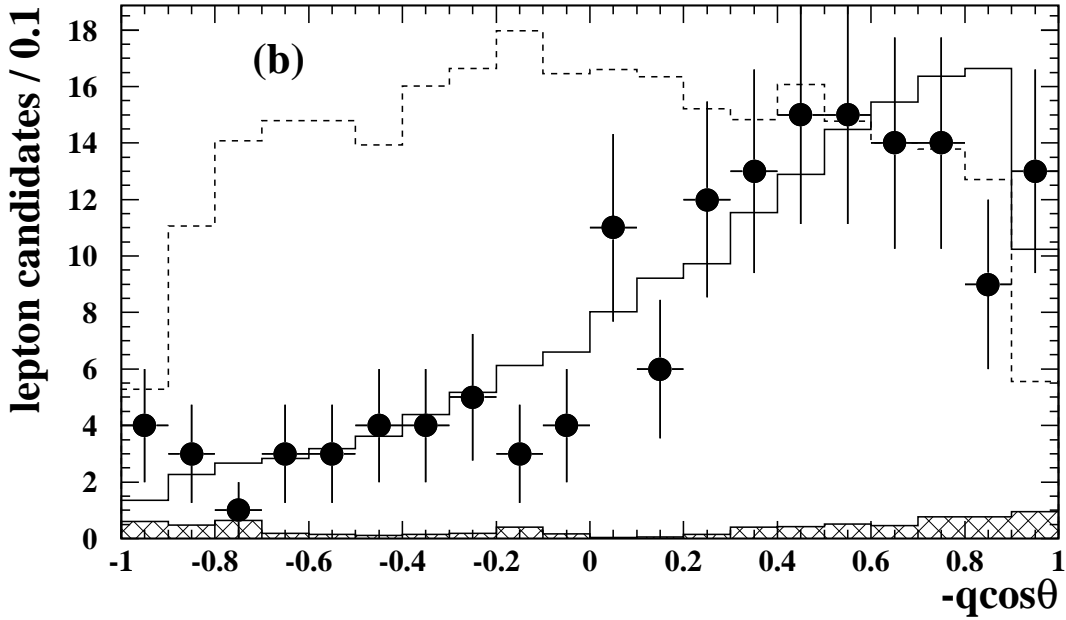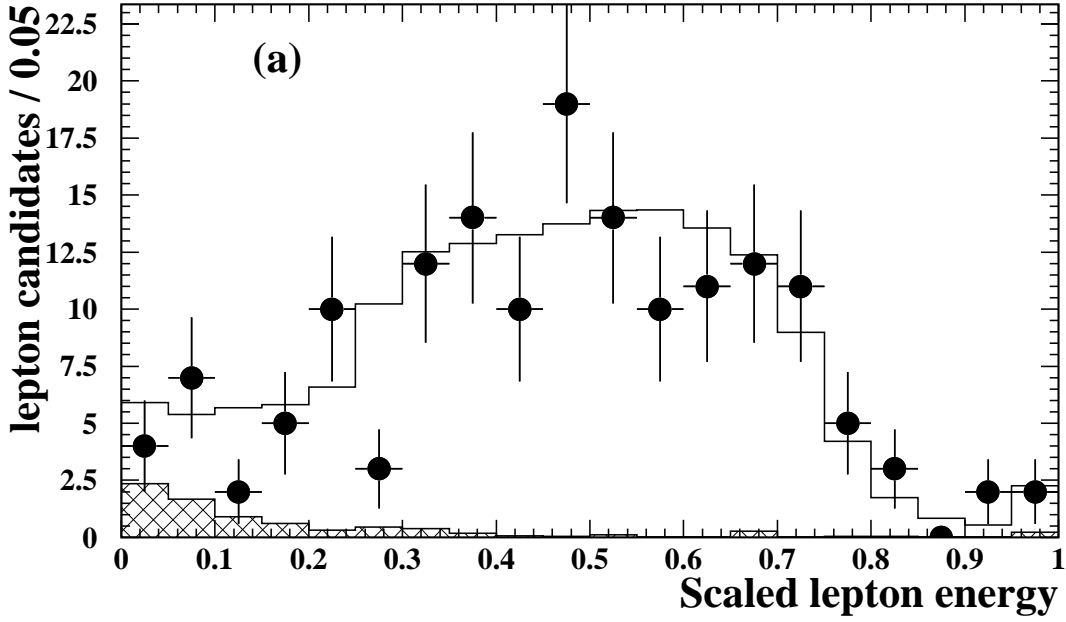
OPAL

Figure 1: *Distributions of (a) the lepton energy divided by the beam energy, and (b) $-q\cos\theta$ for the general selection at $\sqrt{s} = 183$ GeV. The data are shown as the points with error bars. The Standard Model Monte Carlo prediction for $\ell^+\nu\,\ell^-\overline{\nu}$ is shown as the open histogram and the background, arising mainly from processes with four charged leptons in the final state, is shown as the cross-hatched histogram. In (b) the dashed histogram corresponds to the distribution expected from smuon pair production.*
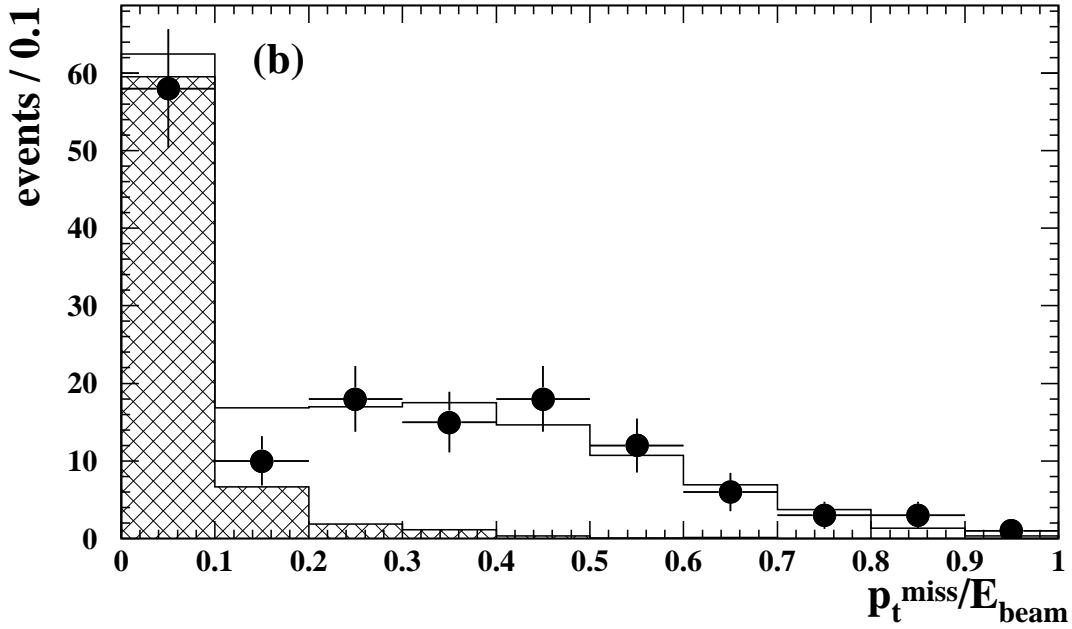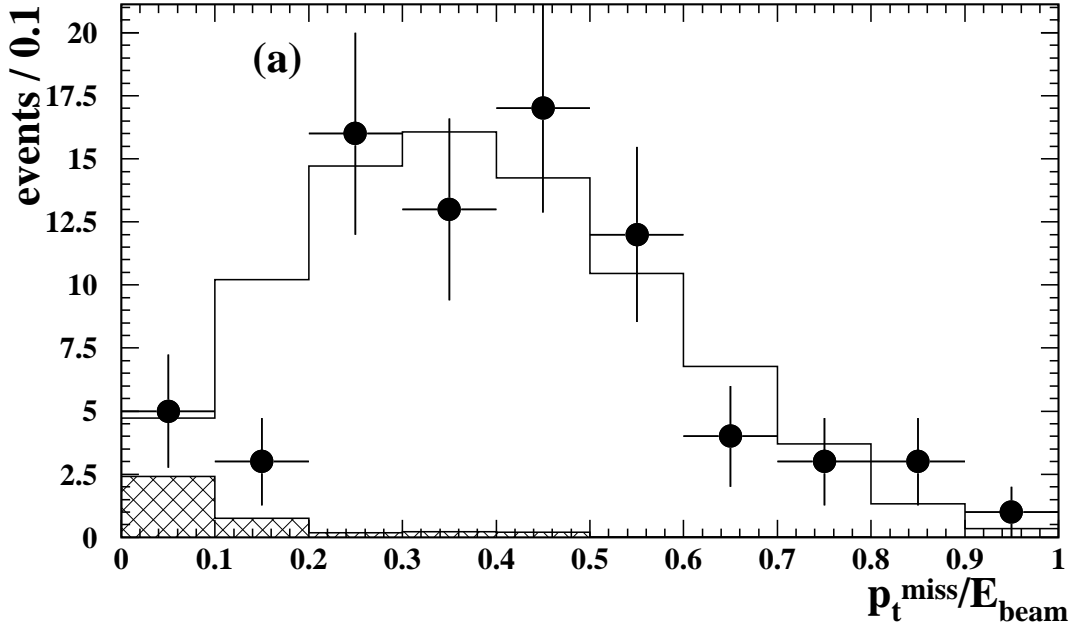
Figure 2: (a) Distribution of $p_t^{\mathrm{miss}}/E_{\mathrm{beam}}$ for the general selection at $\sqrt{s} = 183$ GeV. (b) Distribution of $p_t^{\mathrm{miss}}/E_{\mathrm{beam}}$ at $\sqrt{s} = 183$ GeV for the event sample produced by relaxing some of the selection cuts as described in appendix I.3 of [1]. The data are shown as the points with error bars. The Standard Model Monte Carlo prediction for $\ell^+\nu\,\ell^-\overline{\nu}$ is shown as the open histogram and the background, arising mainly from processes with four charged leptons in the final state, is shown as the cross-hatched histogram.

20
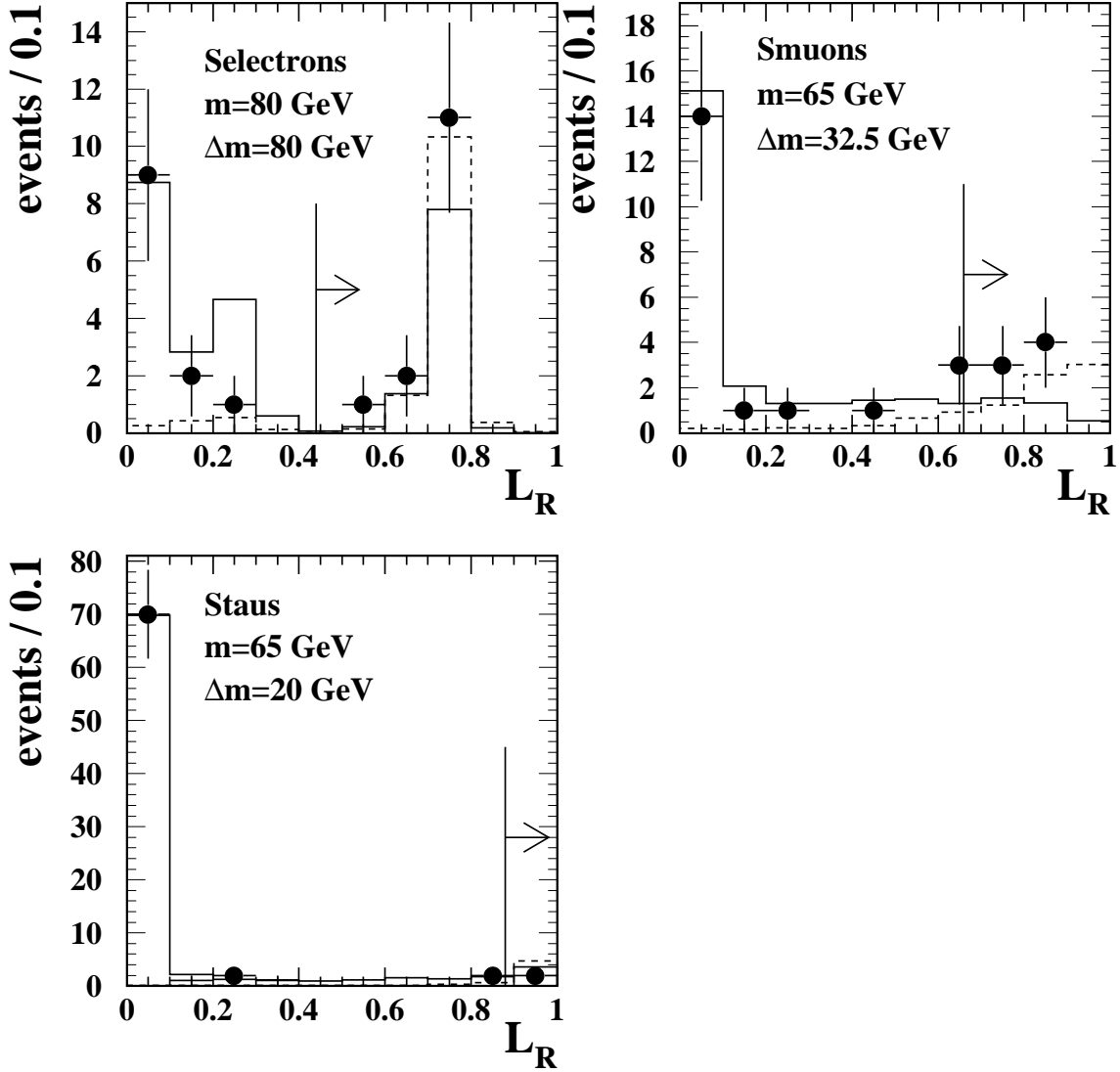
Figure 3: *Distributions of the quantity L_R, defined in section 4, for selectrons, smuons and staus for some specific values of m and Δm at $\sqrt{s} = 183$ GeV. The data are shown as the points with error bars. The predicted Standard Model background is shown as the solid histogram. The dashed histogram corresponds to the distribution expected from selectron, smuon or stau pair production. The signal distribution is normalised in each case to represent the cross-section times branching ratio squared excluded at 95% CL by this analysis, for the values of m and Δm shown.*

OPAL
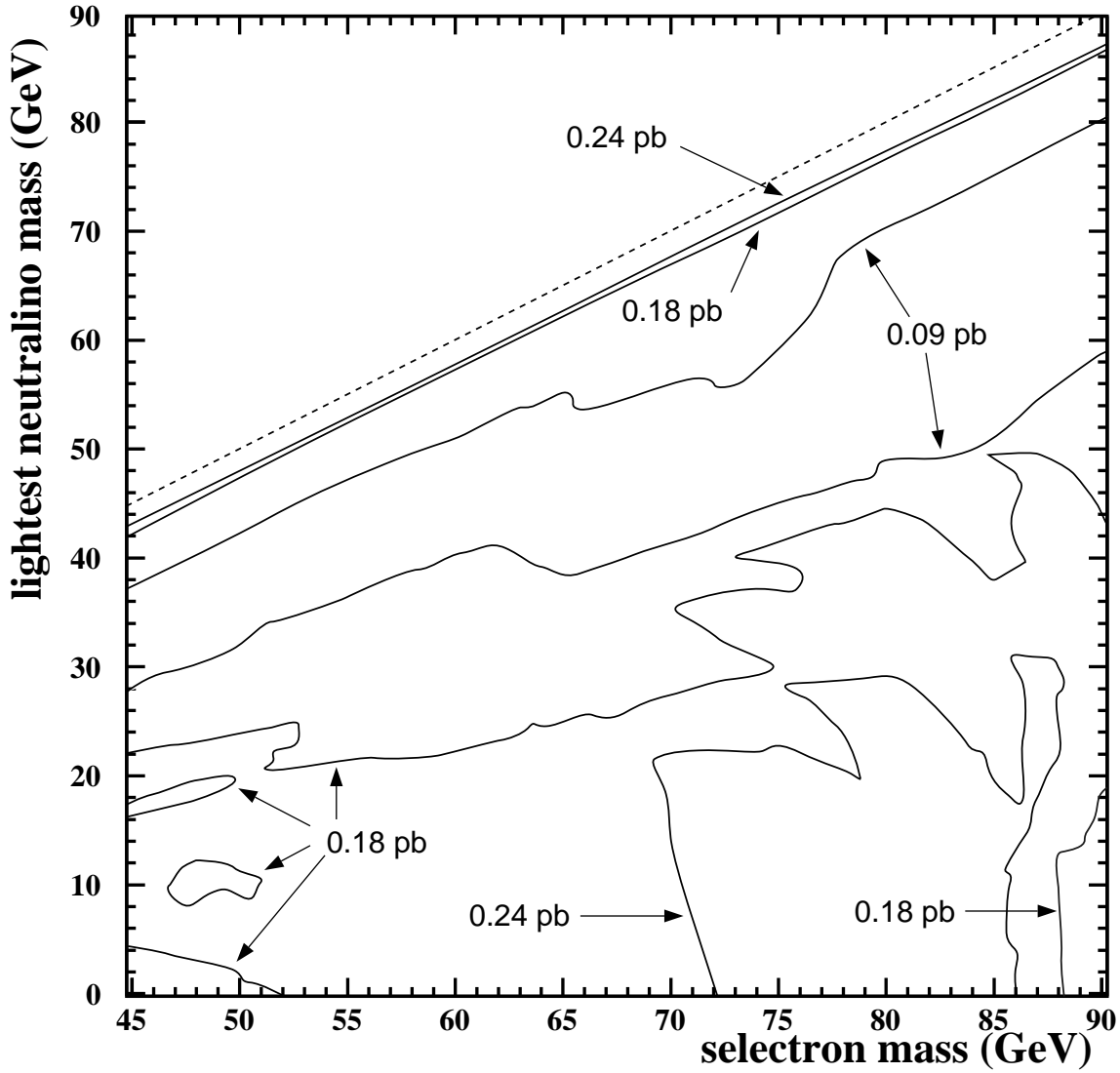
Figure 4: *Contours of the 95% CL upper limits on the selectron pair cross-section times $BR^2(\tilde{e} \to e\tilde{\chi}^0_1)$ at $\sqrt{s} = 183$ GeV based on combining the $\sqrt{s} = 161 - 183$ GeV data-sets assuming a β^3/s dependence of the cross-section. The kinematically allowed region is indicated by the dashed line.*

OPAL
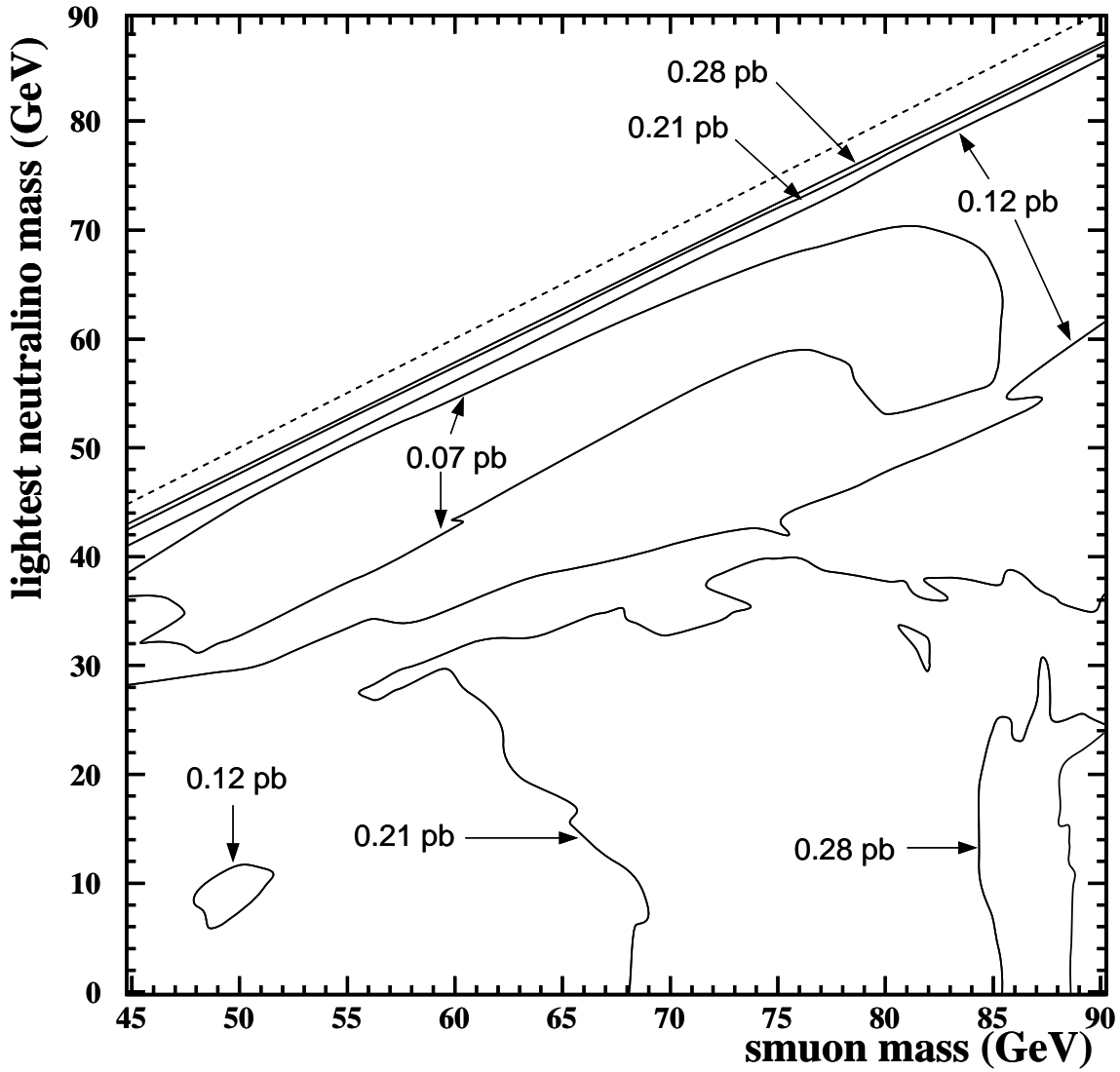
Figure 5: *Contours of the 95% CL upper limits on the smuon pair cross-section times $BR^2(\tilde{\mu} \rightarrow \mu\tilde{\chi}_1^0)$ at $\sqrt{s} = 183$ GeV based on combining the $\sqrt{s} = 161 - 183$ GeV data-sets assuming a β^3/s dependence of the cross-section. The kinematically allowed region is indicated by the dashed line.*
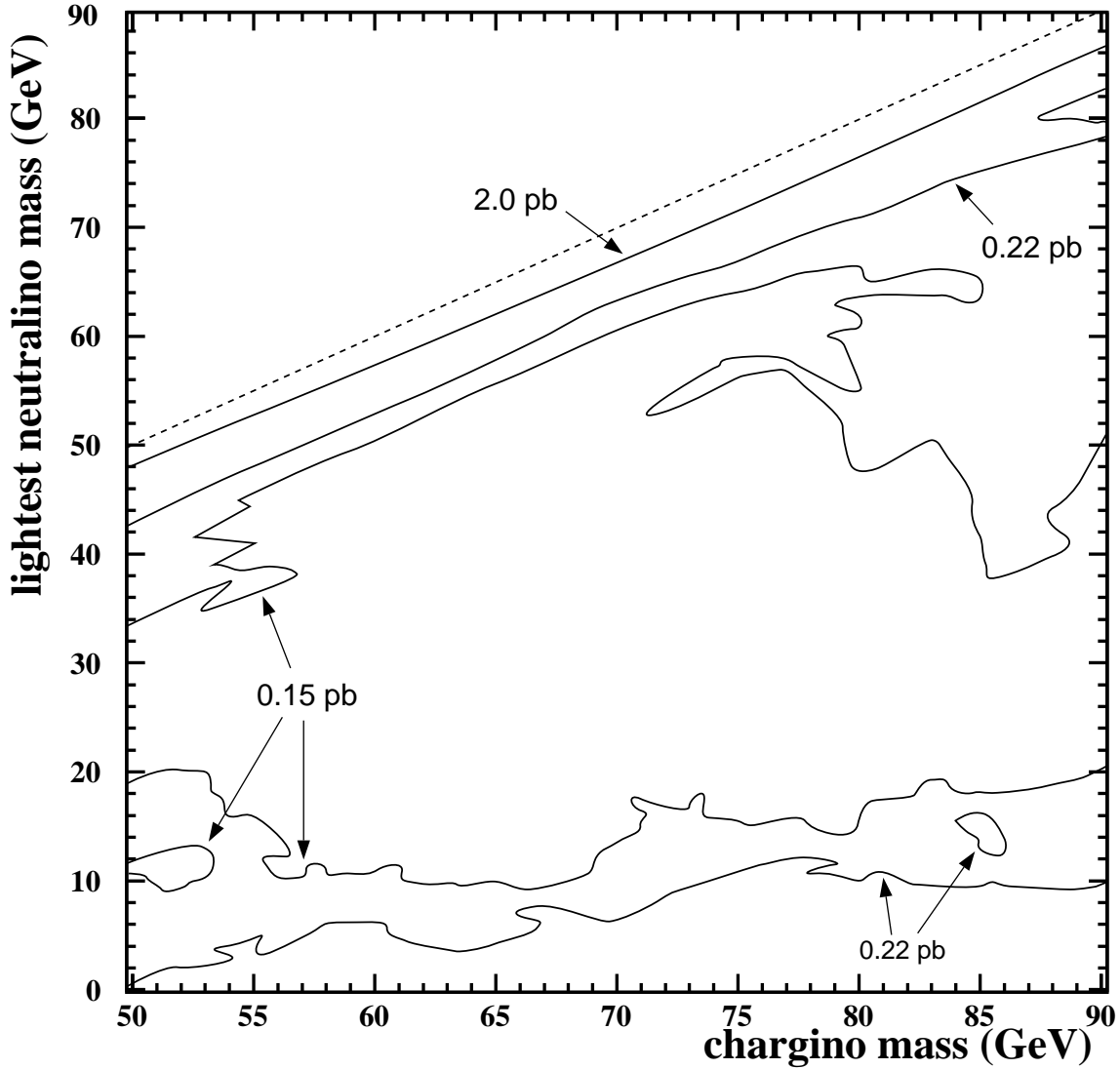
OPAL
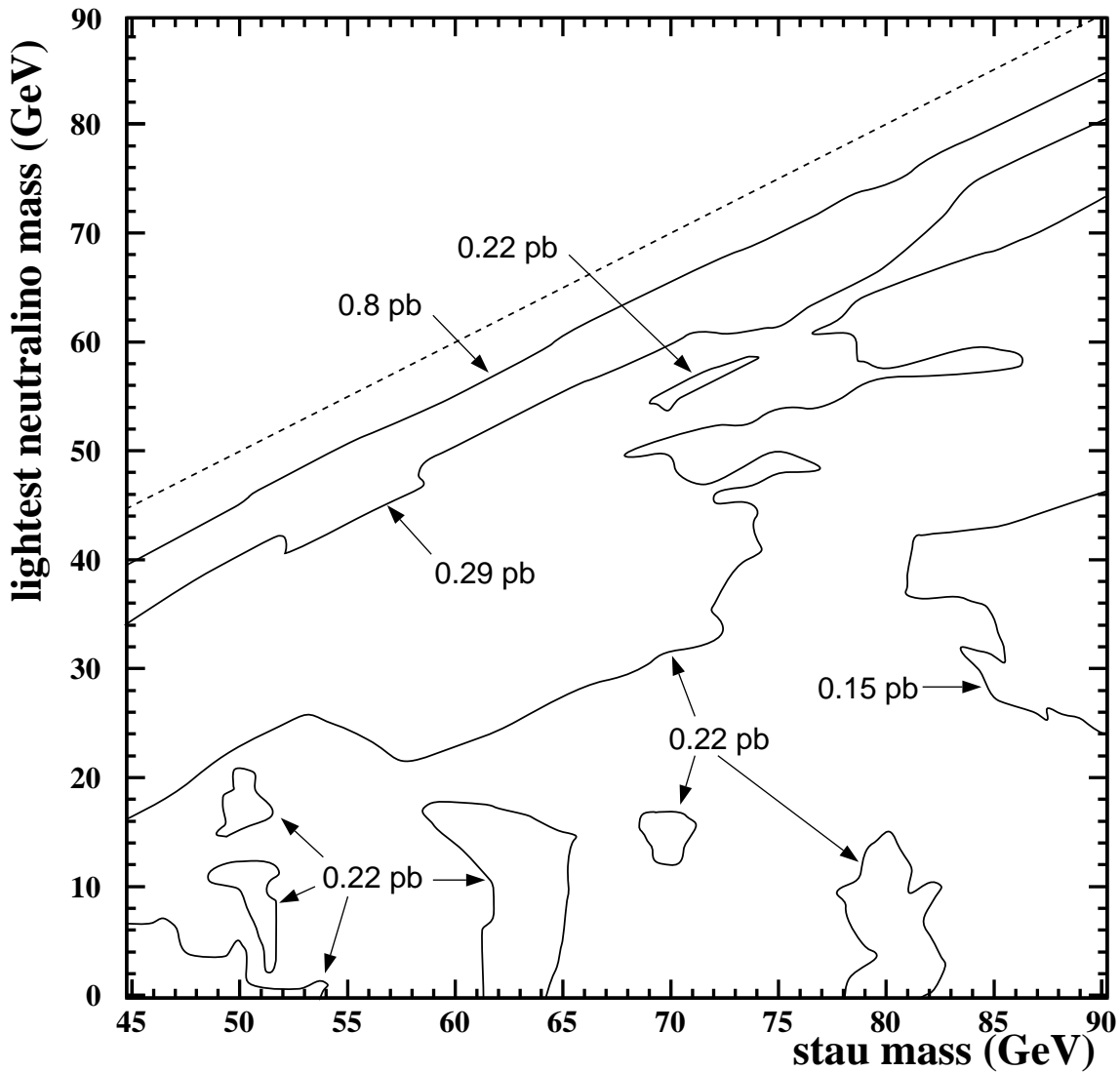
Figure 6: *Contours of the 95% CL upper limits on the stau pair cross-section times $BR^2(\tilde{\tau} \to \tau\tilde{\chi}_1^0)$ at $\sqrt{s} = 183$ GeV based on combining the $\sqrt{s} = 161 - 183$ GeV data-sets assuming a β^3/s dependence of the cross-section. The selection efficiency for $\tilde{\tau}^+\tilde{\tau}^-$ is calculated for the case that the decay $\tilde{\tau}^- \to \tau^-\tilde{\chi}_1^0$ produces unpolarized $\tau^\pm$. The kinematically allowed region is indicated by the dashed line.*

OPAL
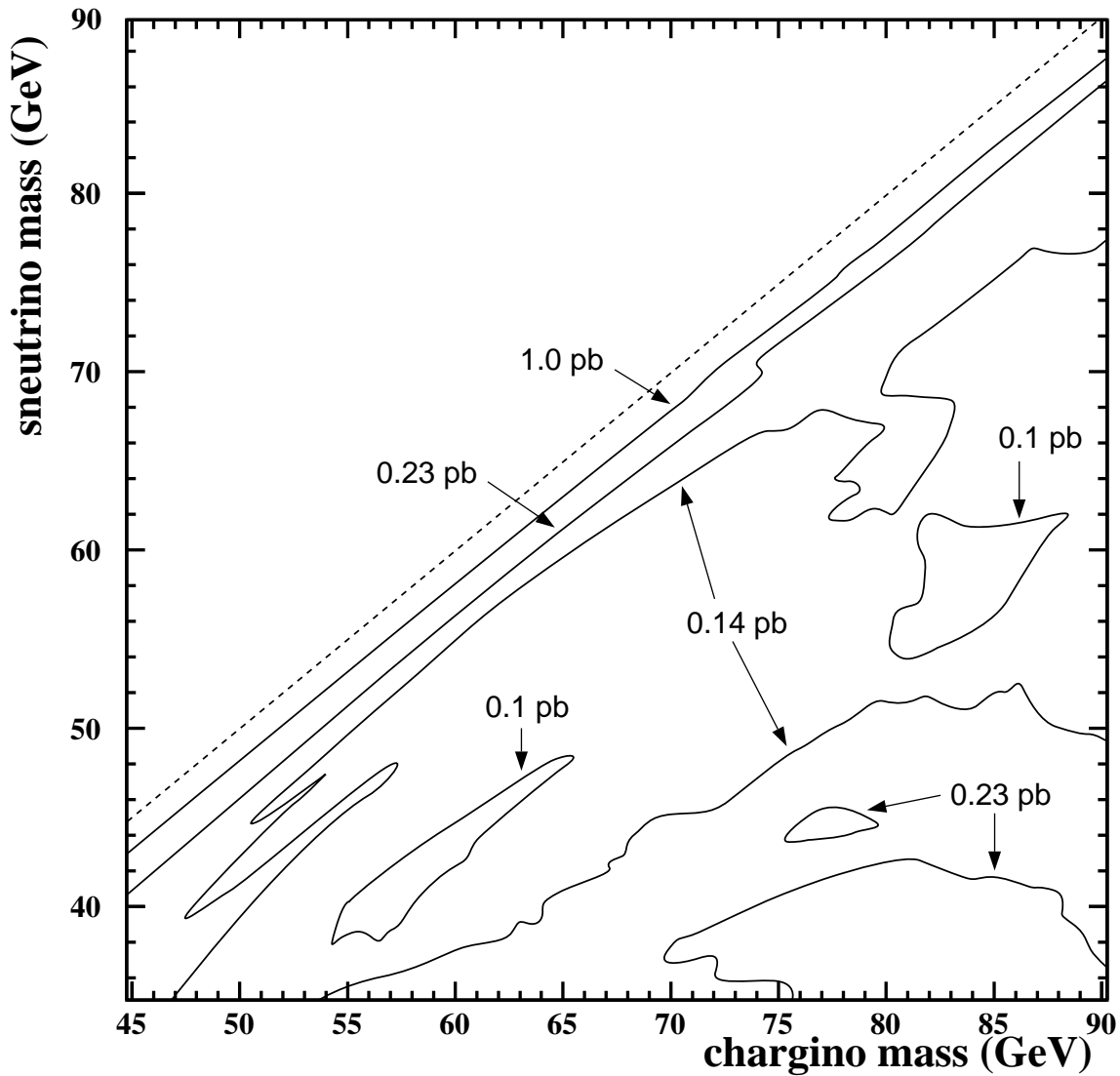
Figure 7: *Contours of the 95% CL upper limits on the chargino pair cross-section times branching ratio squared for* $\tilde{\chi}_1^{\pm} \to \ell^{\pm}\tilde{\nu}$ *(2-body decay) at* $\sqrt{s} = 183$ *GeV. The limits have been calculated for the case where the three sneutrino generations are mass degenerate. The limit is obtained by combining the 161–183 GeV data-sets assuming a* β/s *dependence of the cross-section. The kinematically allowed region is indicated by the dashed line.*

OPAL

Figure 8: *Contours of the 95% CL upper limits on the chargino pair cross-section times branching ratio squared for $\tilde{\chi}_1^{\pm} \to \ell^{\pm} \nu \tilde{\chi}_1^0$ (3-body decay) at $\sqrt{s} = 183$ GeV, The limit is obtained by combining the 161–183 GeV data-sets assuming a β/s dependence of the cross-section. The kinematically allowed region is indicated by the dashed line.*

OPAL
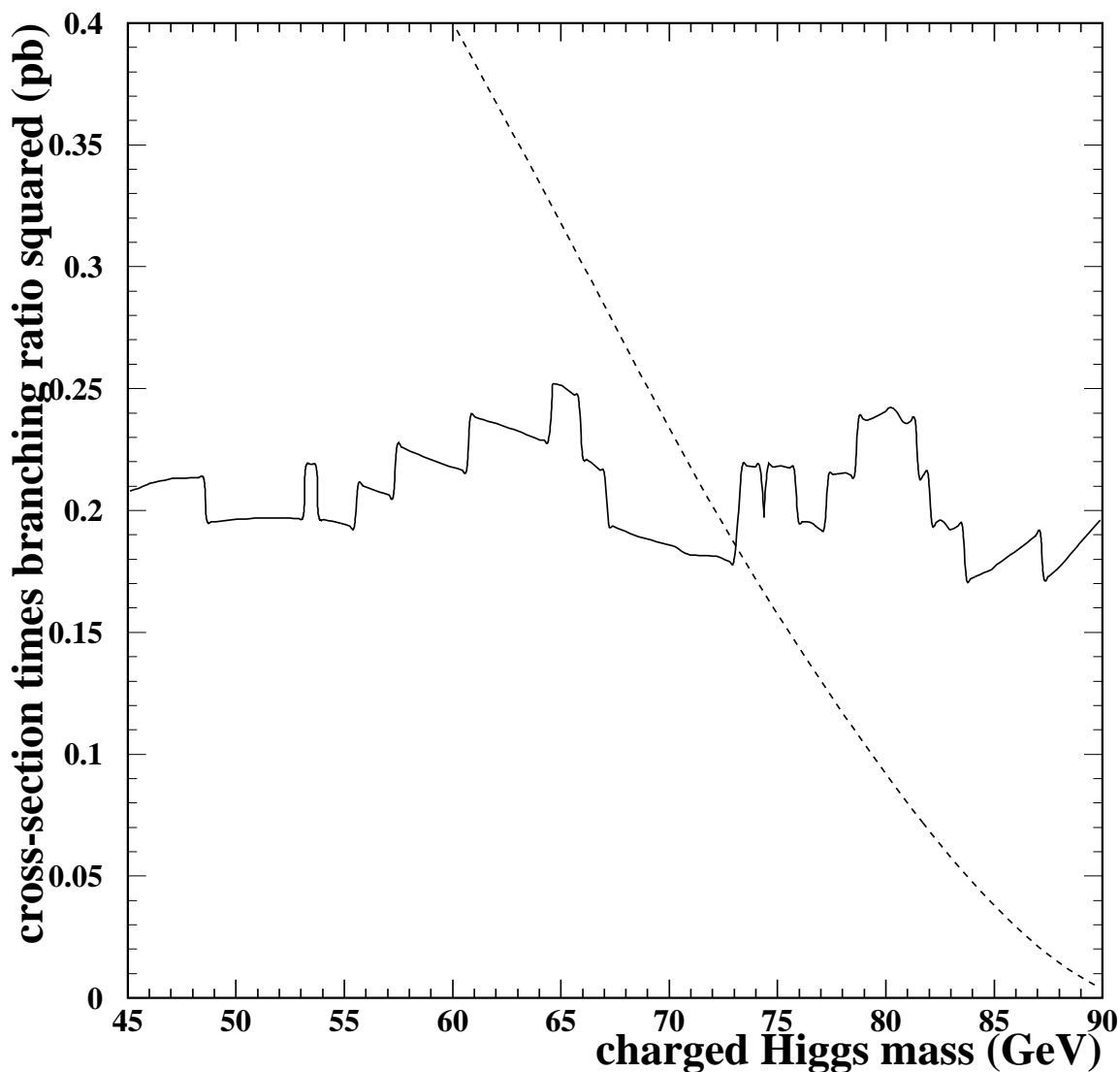
Figure 9: *The solid line shows the 95% CL upper limit on the charged Higgs pair production cross-section times branching ratio squared for the decay $H^+ \to \tau^+ \nu_\tau$ at $\sqrt{s} = 183$ GeV. The limit is obtained by combining the 161–183 GeV data-sets assuming the m_{H^+} and $\sqrt{s}$ dependence of the cross-section predicted by PYTHIA. For comparison, the dashed curve shows the prediction from PYTHIA at $\sqrt{s} = 183$ GeV assuming a 100% branching ratio for the decay $H^+ \to \tau^+ \nu_\tau$.*
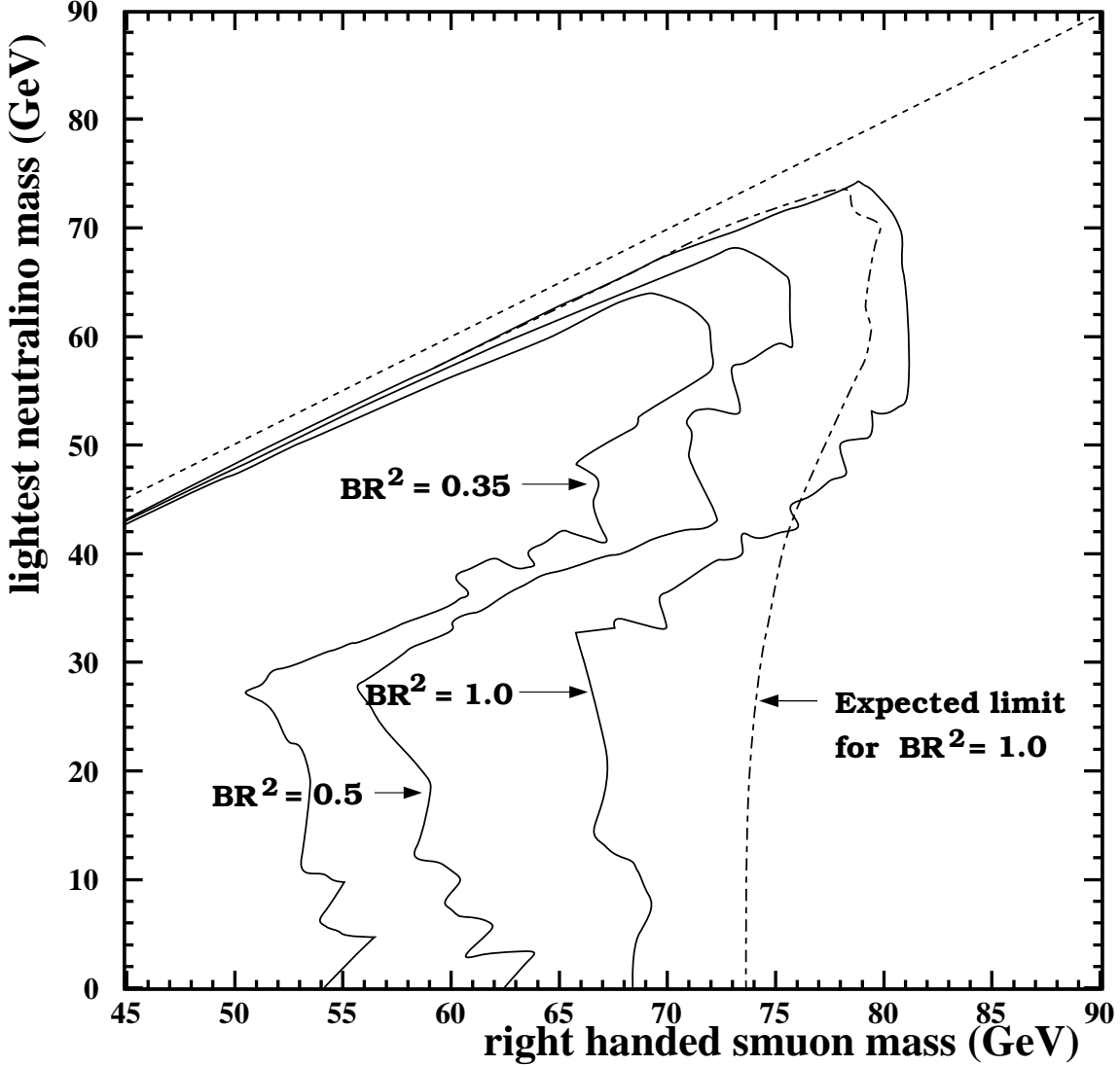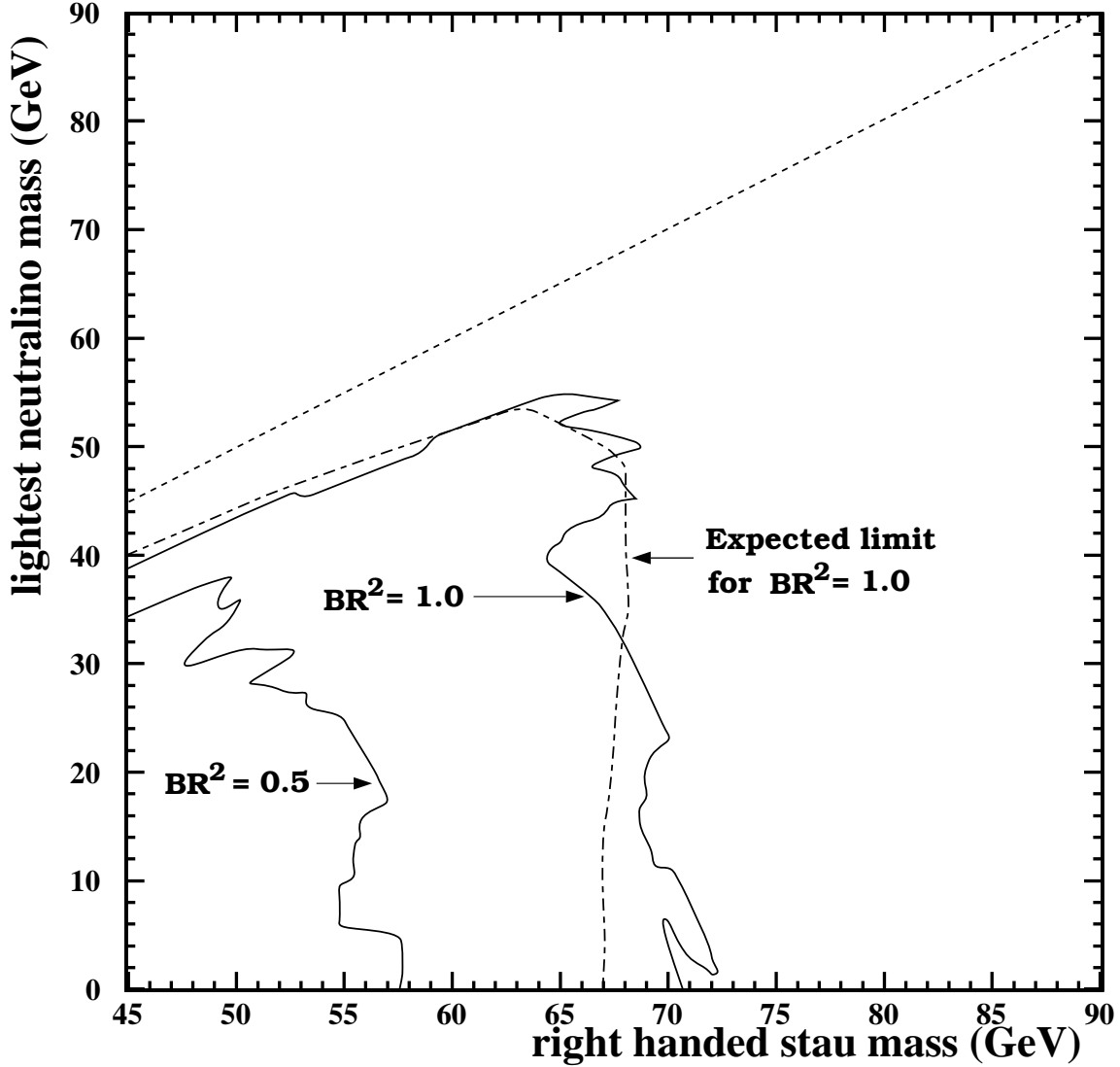
Figure 10: *95% CL exclusion region for right-handed smuon pair production obtained by combining the $\sqrt{s} = 161 - 183$ GeV data-sets. The limits are calculated for several values of the branching ratio squared for $\tilde{\mu}_R^{\pm} \to \mu^{\pm} \tilde{\chi}_1^0$ that are indicated in the figure. Otherwise they have no supersymmetry model assumptions. The kinematically allowed region is indicated by the dashed line. The expected limit for $BR^2 = 1.0$, calculated from Monte Carlo alone, is indicated by the dash-dotted line.*

OPAL

Figure 11: *95% CL exclusion region for right-handed stau pair production obtained by combining the $\sqrt{s} = 161 - 183$ GeV data-sets. The limits are calculated for two values of the branching ratio squared for $\tilde{\tau}_R^{\pm} \rightarrow \tau^{\pm} \tilde{\chi}_1^0$. The selection efficiency for $\tilde{\tau}^+ \tilde{\tau}^-$ is calculated for the case that the decay $\tilde{\tau}^- \rightarrow \tau^- \tilde{\chi}_1^0$ produces unpolarized $\tau^{\pm}$. Otherwise the limits have no supersymmetry model assumptions. The kinematically allowed region is indicated by the dashed line. The expected limit for $BR^2 = 1.0$, calculated from Monte Carlo alone, is indicated by the dash-dotted line.*
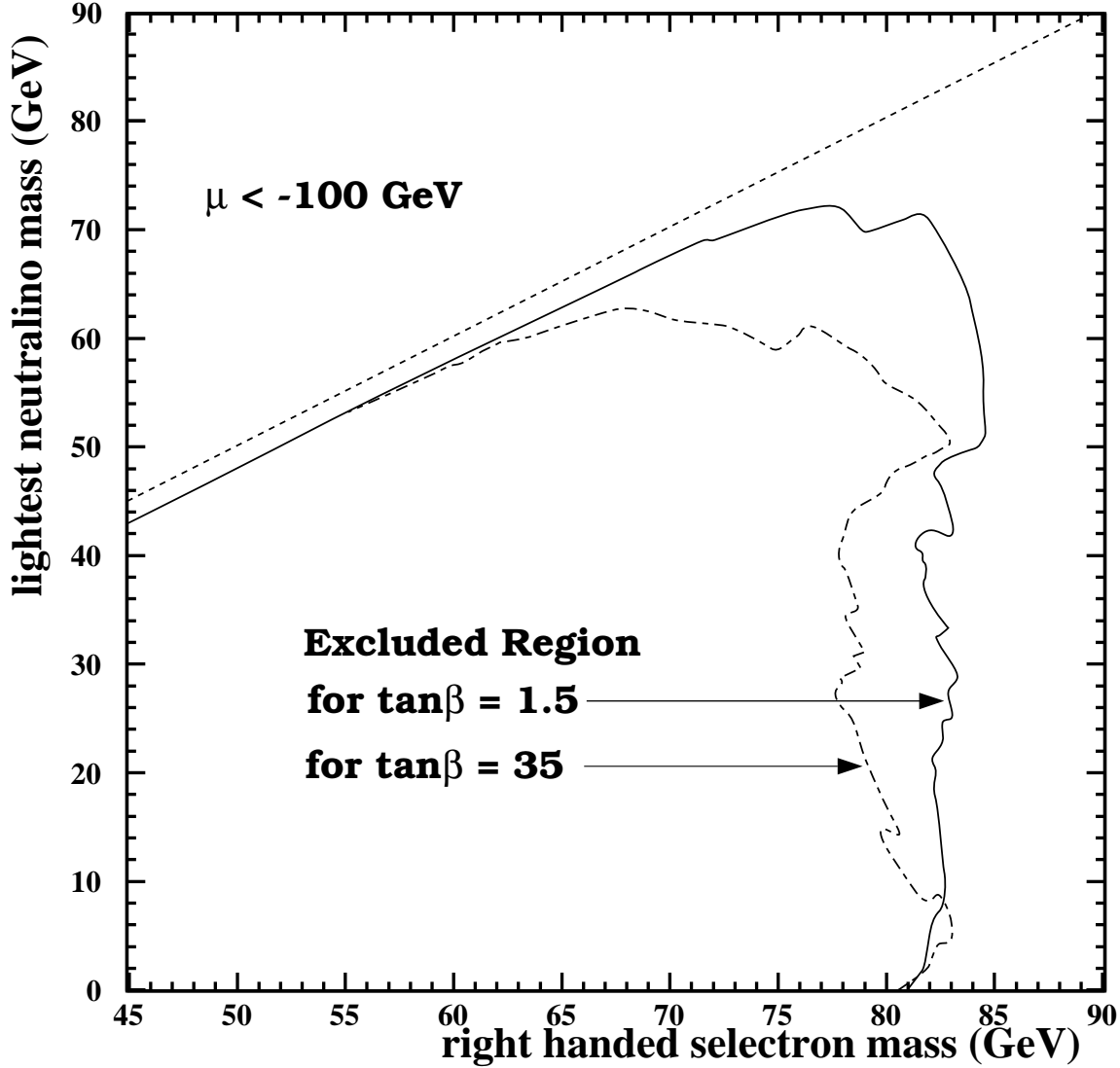
OPAL

Figure 12: *For two values of* $\tan \beta$ *and* $\mu < -100$ *GeV, 95% CL exclusion regions for right-handed selectron pairs within the MSSM, obtained by combining the* $\sqrt{s} = 161-183$ *GeV data-sets. The excluded regions are calculated taking into account the predicted branching ratio for* $\tilde{e}_R^{\pm} \to e^{\pm} \tilde{\chi}_1^0$. *The gauge unification relation,* $M_1 = \frac{5}{3} \tan^2 \theta_W M_2$, *is assumed in calculating the MSSM cross-sections and branching ratios. The kinematically allowed region is indicated by the dashed line.*
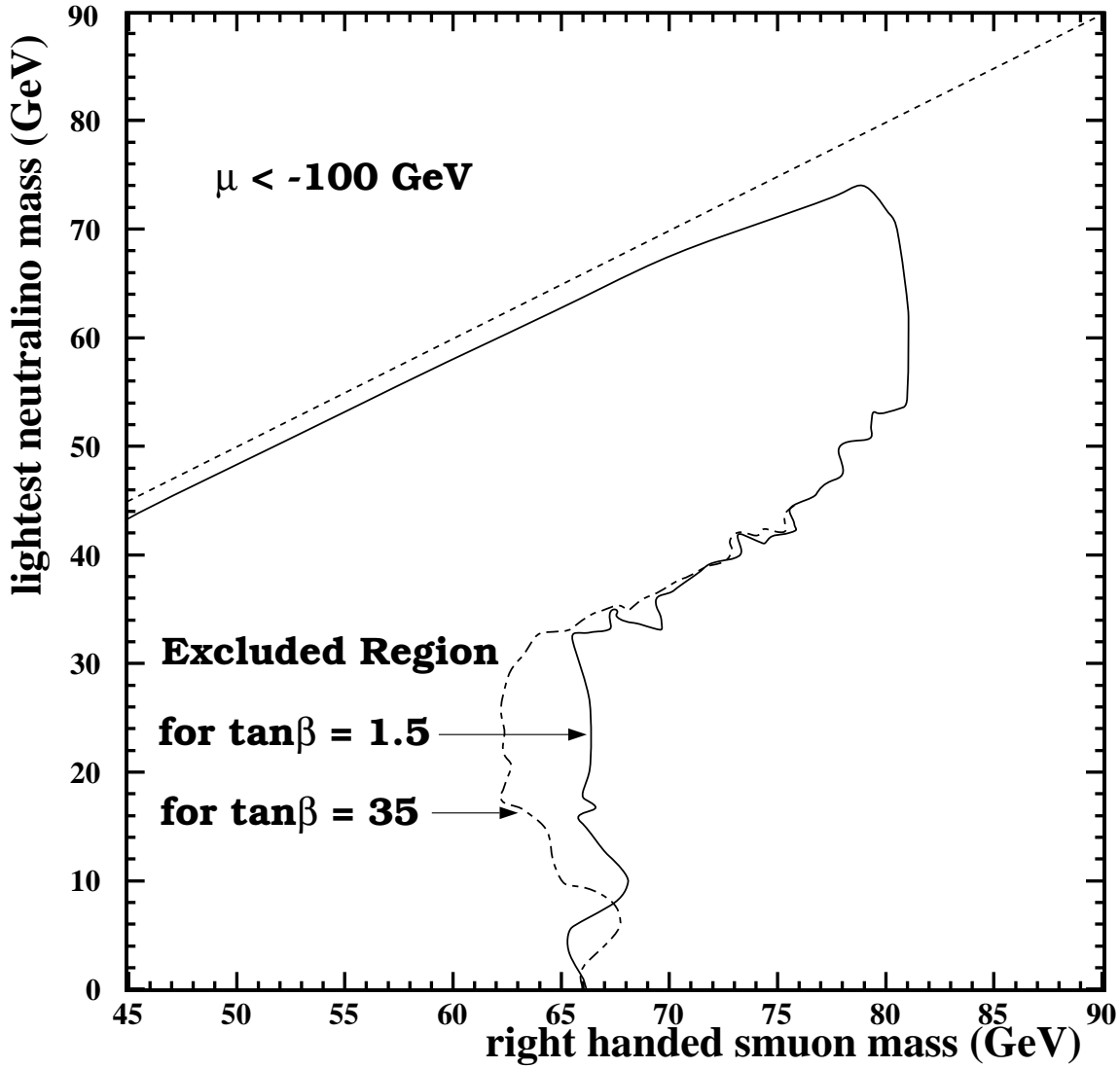
OPAL

Figure 13: *For two values of* $\tan\beta$ *and* $\mu < -100$ *GeV, 95% CL exclusion regions for right-handed smuon pairs within the MSSM, obtained by combining the* $\sqrt{s} = 161 - 183$ *GeV data-sets. The excluded regions are calculated taking into account the predicted branchingz ratio for* $\tilde{\mu}_R^\pm \to \mu^\pm \tilde{\chi}_1^0$. *The gauge unification relation,* $M_1 = \frac{5}{3}\tan^2\theta_W M_2$, *is assumed in calculating the MSSM branching ratios. The kinematically allowed region is indicated by the dashed line.*
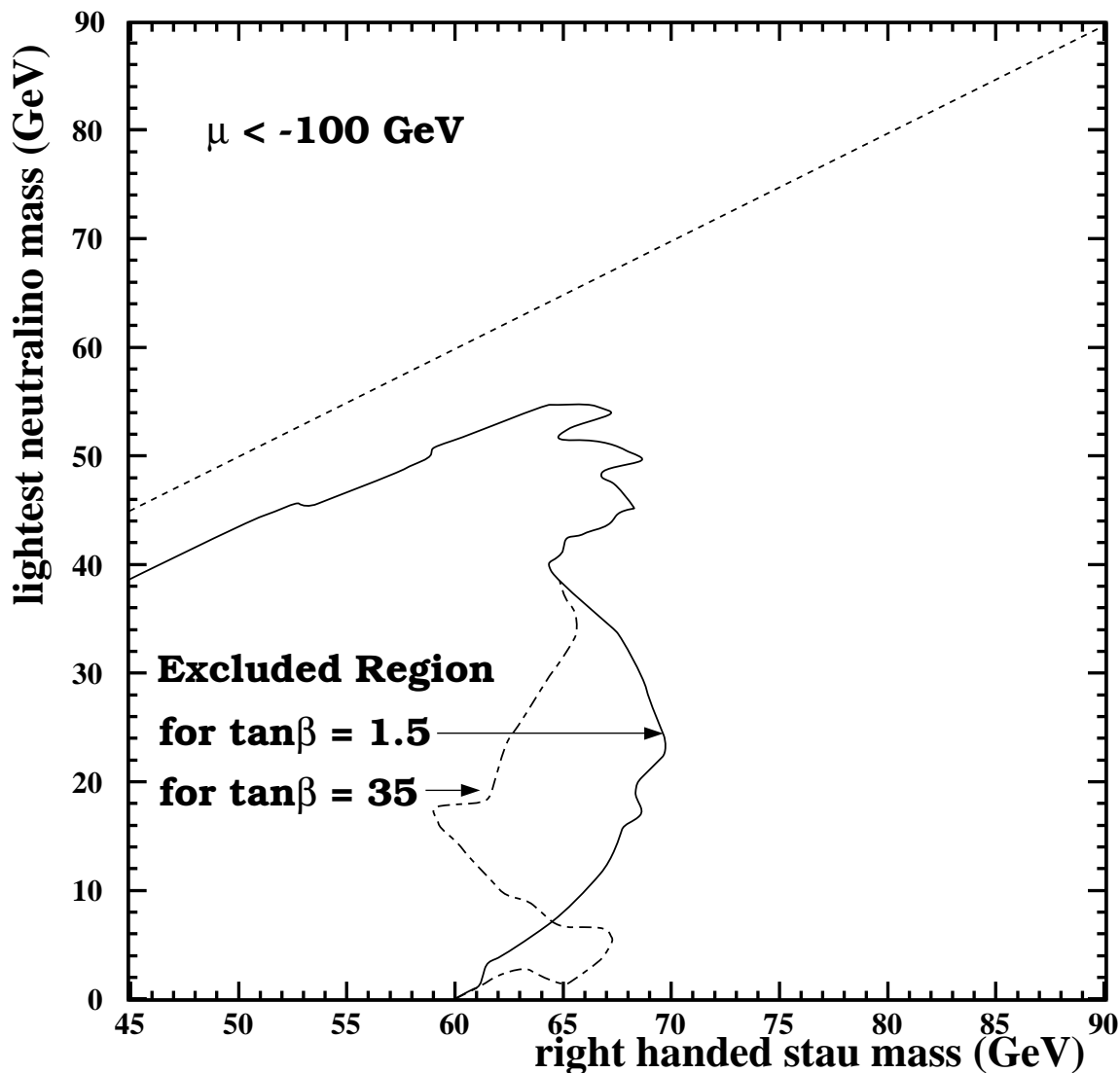
OPAL

Figure 14: *For two values of* $\tan\beta$ *and* $\mu < -100$ *GeV, 95% CL exclusion regions for right-handed stau pairs within the MSSM, obtained by combining the* $\sqrt{s} = 161 - 183$ *GeV data-sets. The excluded regions are calculated taking into account the predicted branching ratio for* $\tilde{\tau}_R^{\pm} \to \tau^{\pm}\tilde{\chi}_1^0$. *The gauge unification relation,* $M_1 = \frac{5}{3}\tan^2\theta_W M_2$, *is assumed in calculating the MSSM branching ratios. The selection efficiency for* $\tilde{\tau}^+\tilde{\tau}^-$ *is calculated for the case that the decay* $\tilde{\tau}^- \to \tau^-\tilde{\chi}_1^0$ *produces unpolarized* $\tau^{\pm}$. *The kinematically allowed region is indicated by the dashed line.*